

$\mathcal{N} = 2^*$ de Sitter vacuum from localization?

Alex Buchel

*Department of Applied Mathematics
Department of Physics and Astronomy
University of Western Ontario
London, Ontario N6A 5B7, Canada
Perimeter Institute for Theoretical Physics
Waterloo, Ontario N2J 2W9, Canada*

Abstract

Holographic correspondence is used to study properties of dS_4 vacuum of mass deformed $\mathcal{N} = 4$ supersymmetric Yang-Mills theory — the $\mathcal{N} = 2^*$ gauge theory. Upon analytical continuation $dS_4 \rightarrow S^4$ the model (with appropriate background space-time curvature coupling) has $\mathcal{N} = 2$ supersymmetry and is mapped by supersymmetric localization to a zero-dimensional matrix model. The resulting matrix model can be solved analytically in the planar limit and perturbatively at large 't Hooft coupling. This led to precision tests of holography for the partition function of $\mathcal{N} = 2^*$ gauge theory and the expectation value of its supersymmetric Wilson loop. We present the holographic prediction for the entropy density of the de Sitter vacuum of the theory. The challenge remains to understand this quantity, its physical origin, from the supersymmetric localization.

April 22, 2019

Contents

1	Introduction	2
2	$\mathcal{R}^{\mathcal{N}=4} = \mathcal{R}_{(0,0)}^{\mathcal{N}=2^*} = 0$	6
2.1	$\mathcal{N} = 4$ SYM perspective	9
2.2	Holographic dual perspective	9
2.3	$\mathcal{N} = 4$ SYM de Sitter late-time vacuum	11
3	$\mathcal{R}_{(m,k)}^{\mathcal{N}=2^*}$	12
3.1	BEFP and PW effective actions	14
3.2	$\mathcal{R}_{(m=i\mu, k=\mu H/2)}^{\mathcal{N}=2^*}$ and $\mathcal{R}_{(m=\mu, k=i\mu H/2)}^{\mathcal{N}=2^*}$	16
3.3	$\mathcal{R}_{(m=\mu, k=\mu H/2)}^{\mathcal{N}=2^*}$	22
4	Discussion	25
4.1	s_{ent} as a thermal entropy of pair-produced particles	27
4.2	s_{ent} as a thermodynamic entropy of the localization free energy at $T = T_{dS}$	29
A	BEFP equations of motion	31
B	$(m, k) = (i\mu, \mu/2)$ equations of motion	32
C	$(m, k) = (\mu, \mu/2)$ equations of motion	33
D	IR thermodynamics of $\mathcal{N} = 2^*$ plasma	33

1 Introduction

The fundamental problem is understanding the current accelerated expansion of the Universe [1, 2]. A positive cosmological constant is the most straightforward explanation, however it implies that we live in (asymptotically) de Sitter space-time. Whether or not de Sitter vacua are consistent in quantum gravity (String Theory) is an active area of research [3, 4].

In this paper we do not study quantum de Sitter gravity, rather, we focus on a much simpler problem — unambiguous¹ signatures of a QFT in classical de Sitter background

¹A vacuum energy of a QFT in dS_4 is *not* unambiguous — it is renormalization scheme dependent, which is one facet of the cosmological constant problem.

space-time. An observable of interest here is the entropy density of a QFT in de Sitter vacuum. We begin reviewing the argument, established in the context of Maldacena duality [5, 6] in [7], that a non-conformal gauge theory in de Sitter space-time (flat or closed spatial slicing),

$$ds_4^2 = -dt^2 + e^{2Ht} d\mathbf{x}^2 \quad \text{or} \quad ds_4^2 = -dt^2 + \frac{1}{H^2} \cosh^2(Ht) (dS^3)^2, \quad (1.1)$$

approaches at late-times a non-equilibrium vacuum state, characterized by a constant rate \mathcal{R} of the comoving entropy production

$$\lim_{t \rightarrow \infty} \frac{1}{H^3 a^3} \frac{d}{dt} (a^3 s) \equiv 3H \times \mathcal{R}, \quad (1.2)$$

where $a = e^{Ht}$ or $a = \cosh(Ht)/H$ is the scale factor. The rate \mathcal{R} , unlike the stress-energy tensor of the theory, is renormalization scheme unambiguous. It depends on QFT scales (physical mass parameters and relevant renormalizable coupling constants) breaking the conformal invariance; furthermore, in the limit where the scale invariance is restored,

$$\lim_{QFT \rightarrow CFT} \mathcal{R} = 0, \quad (1.3)$$

in agreement with the adiabaticity of the (Euclidean) de Sitter CFT vacuum. Eq. (1.2) suggests a simple physical meaning of the rate \mathcal{R} [8]:

$$\lim_{t \rightarrow \infty} s \equiv s_{ent} = H^3 \mathcal{R}. \quad (1.4)$$

Even though the late-time de Sitter state can be assigned (from the holographic perspective) a Hawking temperature

$$T_{dS} = \frac{H}{2\pi}, \quad (1.5)$$

s_{ent} can not be a thermal entropy of the QFT at $T = T_{dS}$. This is evident from the fact (using (1.3)) that²

$$s_{thermal}^{CFT} \Big|_{T=T_{dS}} \propto H^3 \quad \text{while} \quad s_{ent}^{CFT} \propto \mathcal{R}^{CFT} = 0. \quad (1.6)$$

In this paper we focus on a precise holographic correspondence between $\mathcal{N} = 2^*$ gauge theory and Pilch-Warner (PW) geometry of type IIB supergravity [9–11]. There are two reasons for this particular choice:

²We return to this in section 4.

■ $\mathcal{N} = 2^*$ theory is a deformation of $\mathcal{N} = 4$ $SU(N)$ supersymmetric Yang-Mills theory. Specifically, in the $\mathcal{N} = 2$ language³, the field content of the latter includes a vector multiplet (a gauge field A_μ , two Weyl fermions ψ_1 and ψ_2 and a complex scalar Z_3) and a hypermultiplet consisting of two complex scalar fields Z_1 and Z_2 and two Weyl fermions χ_1 and χ_2 . The mass deformation that results in $\mathcal{N} = 2^*$ gauge theory is a mass term for the hypermultiplet:

$$\mathcal{L}_{\mathcal{N}=2^*} = \mathcal{L}_{\mathcal{N}=4} + m^2 \text{Tr} (|Z_1|^2 + |Z_2|^2) + m \text{Tr} (\chi_1 \chi_1 + \chi_2 \chi_2 + \text{h.c.}) . \quad (1.7)$$

As a result, as it was already shown in [7],

$$\mathcal{R}^{\mathcal{N}=2^*} \neq 0 . \quad (1.8)$$

■ The second reason is an attempt to exploit the precision holography in a non-conformal setting in the context of large- N $\mathcal{N} = 2^*$ gauge theory [12–19]. Notice that the Wick rotation of the closed de Sitter geometry is that of the four-sphere

$$-dt^2 + \frac{1}{H^2} \cosh^2(Ht) (dS^3)^2 \quad \underset{t \rightarrow \frac{i}{H}\theta}{\rightleftharpoons} \quad \frac{1}{H^2} (dS^4)^2 , \quad (1.9)$$

of radius $1/H$. While the Poincare supersymmetries are completely broken for $\mathcal{L}_{\mathcal{N}=2^*}$ model on S^4 , $\mathcal{N} = 2$ (Euclidean) supersymmetry can be restored with appropriately tuned curvature coupling⁴ k [13]:

$$\mathcal{L}_{\mathcal{N}=2^*}^{(m,k)} \equiv \mathcal{L}_{\mathcal{N}=2^*} + k \text{Tr} (Z_1^2 + Z_2^2 + \text{h.c.}) , \quad k = \frac{i}{2} mH . \quad (1.10)$$

Moreover, the model $\mathcal{L}_{\mathcal{N}=2^*}^{(m,imH/2)}$ on S^4 upon supersymmetric localization is mapped to a zero dimensional matrix model [13], which can be solved analytically in the large- N limit [14–17, 19], allowing for precision tests of the holographic correspondence. As we already mentioned, the holographic dual to $\mathcal{L}_{\mathcal{N}=2^*}^{(m,0)}$ is a PW type IIB supergravity — the latter can not be a holographic dual to $\mathcal{L}_{\mathcal{N}=2^*}^{(m,k \neq 0)}$: explicit computations of the holographic and the matrix model partition functions on S^4 demonstrated a disagreement [20]. Shortly after the disagreement was pointed out, the correct holographic dual to $\mathcal{L}_{\mathcal{N}=2^*}^{(m,k)}$ was identified [12] (BEFP)⁵. Of course, on the level of the effective actions,

³We use notations of [12].

⁴The S^4 supersymmetry is unique up to a discrete choice represented by $k \rightarrow -k$.

⁵See [18] for a 10d uplift of BEFP geometry.

we have a consistent truncation

$$\text{BEFP} \Big|_{k=0} = \text{PW}. \quad (1.11)$$

The previous computation of the rate (1.8) was performed at $k = 0$, and thus there is no chance of understanding this quantity from the matrix model perspective. This paper is an extension of the computations of [7] to $\mathcal{R}_{(m,k)}^{\mathcal{N}=2^*}$.

We want to stress the following facts:

- We do not understand how to compute $\mathcal{R}_{(m,imH/2)}^{\mathcal{N}=2^*}$ from localization. Neither do we understand the physical origin of the quantity⁶. We present the holographic computations of the quantity $\mathcal{R}_{(m,k)}^{\mathcal{N}=2^*}$ in three cases:

$$\mathcal{R}_{(m=\mu, k=i\mu H/2)}^{\mathcal{N}=2^*}, \quad \mathcal{R}_{(m=i\mu, k=\mu H/2)}^{\mathcal{N}=2^*}, \quad \mathcal{R}_{(m=\mu, k=\mu H/2)}^{\mathcal{N}=2^*}, \quad (1.12)$$

for a real mass parameter μ .

- Notice that the first two examples are related by an analytical continuation of the mass parameter μ , and we hope might be accessible from the matrix model. It is important to emphasize — as we review in details in section 2 — that the entropy density s_{ent} (1.4) appears to be (from the holographic perspective) an intrinsically Lorentzian quantity. This is in contrast to a thermal entropy which can be understood holographically both in Lorentzian and Euclidean signatures (*e.g.*, as an area of the dual black brane event horizon in Eddington-Finkelstein or (analytically continued) Schwarzschild coordinates).

Given [7], the results presented here are not conceptually new and are technical in nature. Thus, we try to allocate to appendices as much details as possible, leaving only the physical aspects. In section 2 we compute \mathcal{R} for $\mathcal{N} = 4$ SYM. Of course the result is “zero” for this theory, but it illustrates the set of holographic tools used in computing \mathcal{R} for more general models. In section 3 we compute (1.12). Since we will perform the computations in a different framework⁷ from the one used in [7], an agreement

$$\mathcal{R}^{\mathcal{N}=2^*} = \mathcal{R}_{(m,0)}^{\mathcal{N}=2^*} \quad (1.13)$$

⁶See section 4 for some comments.

⁷The computational framework developed here is indispensable in understanding the “phase diagram” of late-time de Sitter states in confining models with spontaneous symmetry breaking, such as Klebanov-Strassler gauge theory [21].

is an important test. Finally, in section 4 we present some comments on failed interpretations of s_{ent} .

$$\mathbf{2} \quad \mathcal{R}^{\mathcal{N}=4} = \mathcal{R}_{(0,0)}^{\mathcal{N}=2^*} = 0$$

The purpose of this section is to set up/review holographic tools used to compute \mathcal{R} . We will do it in the simplest context possible, *i.e.*, $\mathcal{N} = 4$ SYM, which allows for a completely analytic discussion. The price we pay is a trivial result,

$$\mathcal{R}^{\mathcal{N}=4} = 0. \tag{2.1}$$

Consider a five-dimensional gravitational dual to $\mathcal{N} = 4$ $SU(N)$ SYM⁸:

$$S_{\mathcal{N}=4} = \frac{1}{16\pi G_5} \int_{\mathcal{M}_5} d^5\xi \sqrt{-g} \left[R + \frac{12}{L^2} \right]. \tag{2.2}$$

In what follows we set⁹ the asymptotic AdS_5 radius $L = 2$, leading to the identification

$$G_5 = \frac{4\pi}{N^2}. \tag{2.3}$$

A generic state of the gauge theory, homogeneous and isotropic in the spatial boundary coordinates $\mathbf{x} = \{x, y, z\}$, leads to a dual gravitational metric ansatz

$$ds_5^2 = 2dt (dr - A dt) + \Sigma^2 d\mathbf{x}^2, \tag{2.4}$$

with the warp factors A, Σ depending only on $\{t, r\}$. Notice that the metric (2.4) is invariant under the residual diffeomorphisms as $r \rightarrow \bar{r} = r - \lambda(t)$ [22]

$$A(t, r) \rightarrow \bar{A}(t, \bar{r}) = A(t, r + \lambda(r)) - \dot{\lambda}(t), \quad \Sigma(t, r) \rightarrow \bar{\Sigma}(t, \bar{r}) = \Sigma(t, r + \lambda(t)). \tag{2.5}$$

From the effective action (2.2) we obtain the following equations of motion:

$$\begin{aligned} 0 &= (d_+ \Sigma)' + 2\Sigma' d_+ \ln \Sigma - \frac{\Sigma}{2}, \\ 0 &= A'' - 6(\ln \Sigma)' d_+ \ln \Sigma + \frac{1}{2}, \end{aligned} \tag{2.6}$$

⁸To further simplify the discussion we will use a consistent truncation to the metric sector only. The discussion is readily extended in the presence of the bulk scalar fields, dual to $\mathcal{N} = 4$ gauge invariant operators, see below. The conclusion is unchanged.

⁹This is done to agree with the conventions in section 3.

as well as the Hamiltonian and the momentum constraint equations:

$$0 = \Sigma'', \quad 0 = d_+^2 \Sigma - 2A\Sigma' - (4A\Sigma' + A'\Sigma)d_+ \ln \Sigma + \Sigma A. \quad (2.7)$$

In (2.5)-(2.7) we denoted $' = \frac{\partial}{\partial r}$, $\dot{} = \frac{\partial}{\partial t}$, and $d_+ = \frac{\partial}{\partial t} + A\frac{\partial}{\partial r}$. Assuming the SYM background metric (for now we keep the scale factor $a(t)$ arbitrary)

$$ds_4^2 = -dt^2 + a(t)^2 d\mathbf{x}^2, \quad (2.8)$$

the bulk metric (2.4) has the near-boundary $r \rightarrow \infty$ asymptotic behavior

$$\Sigma = \frac{ar}{2} + \mathcal{O}(r^0), \quad A = \frac{r^2}{8} + \mathcal{O}(r^1). \quad (2.9)$$

The most general solution to (2.6)-(2.7), subject to the boundary conditions (2.9) takes form

$$A = \frac{(r + \lambda)^2}{8} - (r + \lambda) \frac{\dot{a}}{a} - \dot{\lambda} - \frac{r_0^4}{8a^4(r + \lambda)^2}, \quad \Sigma = \frac{(r + \lambda)a}{2}, \quad (2.10)$$

where $\lambda(t)$ is an arbitrary function, as in (2.5), and r_0 is a constant. Without loss of generality we now set $\lambda(t) \equiv 0$.

The bulk metric (2.4) has an apparent horizon (AH)¹⁰ at $r = r_{AH}$ where [22]

$$d_+ \Sigma \Big|_{r=r_{AH}} = 0 \quad \implies \quad r_{AH} = \frac{r_0}{a(t)}. \quad (2.11)$$

Following [23, 24] we associate the non-equilibrium (comoving) entropy density $a^3 s$ of the SYM with the Bekenstein-Hawking entropy density of the apparent horizon

$$a^3 s = \frac{\Sigma^3}{4G_5} \Big|_{r=r_{AH}} = \frac{N^2 r_0^3}{128\pi}. \quad (2.12)$$

Further, from [25] we identify the surface gravity κ_{suf} of the dynamical AH:

$$\kappa_{suf} = A' \Big|_{r=r_{AH}} = \frac{r_0}{2a(t)} - \frac{d}{dt} \ln a(t). \quad (2.13)$$

For a stationary horizon the surface gravity is constant, and one identifies the Hawking temperature as

$$T = \frac{\kappa_{suf}}{2\pi}. \quad (2.14)$$

¹⁰In general AH is observer dependent. It is natural to definite AH with respect to an observer reflecting the symmetries of the spatial slices — homogeneity and isotropy in \mathbf{x} here. Note that as $t \rightarrow \infty$, which is the limit where we define the entropy production rate \mathcal{R} (1.2), the AH coincides with the event horizon.

Here, we are having a dynamical (non-equilibrium) horizon, and temperature is not well-defined — instead we define local temperature as

$$T_{loc}(t) \equiv \lim_{\dot{a} \rightarrow 0} \frac{\kappa_{suf}}{2\pi} = \frac{r_0}{2a(t)} \equiv \frac{T_0}{a(t)}, \quad (2.15)$$

where $T_0 \equiv r_0/2$. Notice that if the metric (2.8) expansion rate is positive, the local temperature redshifts as expected for a thermal state of a conformal theory. While the comoving entropy density (2.12) is time-independent, the physical entropy density "dilutes":

$$s(t) = \frac{\pi^2}{2} N^2 T_{loc}^3, \quad (2.16)$$

again, as one would expect for a thermal state of $\mathcal{N} = 4$ SYM plasma in FLRW Universe (2.8). It is straightforward to compute the stress-energy momentum tensor; one finds for the energy density \mathcal{E} and the pressure P [7]

$$\mathcal{E}(t) = \frac{3}{8} \pi^2 N^2 T_{loc}^4 + \frac{3N^2}{32\pi^2} \frac{(\dot{a})^4}{a^4}, \quad P(t) = \frac{1}{3} \mathcal{E}(t) - \frac{N^2}{8\pi^2} \frac{(\dot{a})^2 \ddot{a}}{a^3}. \quad (2.17)$$

As expected [7]:

- the stress-energy tensor is conserved as a consequence of the bulk momentum constraint (2.7)

$$\frac{d\mathcal{E}}{dt} + 3\frac{\dot{a}}{a}(\mathcal{E} + P) = 0; \quad (2.18)$$

- the energy density and the pressure are just conformal transformations of the equilibrium thermal state (with $T_{loc} \rightarrow T_0$), properly accounting for the conformal anomaly;
- the trace anomaly is

$$-\mathcal{E} + 3P = \frac{N^2}{32\pi^2} \left(R_{\mu\nu} R^{\mu\nu} - \frac{1}{3} R^2 \right) = -\frac{3N^2}{8\pi^2} \frac{(\dot{a})^2 \ddot{a}}{a^3}. \quad (2.19)$$

We now discuss the late-time dynamics of the model in de Sitter space-time (1.1), from the SYM perspective, and from the bulk geometry perspective. Finally, we outline how the results can be obtained bypassing the construction of dynamical solution and focusing on the late-time limit directly. The latter makes an argument why (2.1) is true for more general states of the SYM, *e.g.*, the states where some operators of the SYM (bulk scalars) are initially excited.

2.1 $\mathcal{N} = 4$ SYM perspective

We take

$$a(t) = e^{Ht}. \quad (2.20)$$

The local temperature of the plasma is given by (2.15), the entropy density is given by (2.16), the energy density and the pressure are given by (2.17). At late times we find

$$\lim_{t \rightarrow \infty} \begin{pmatrix} T_{loc} \\ \mathcal{E} \\ P \\ a^3 s \end{pmatrix} = \begin{pmatrix} 0 \\ \frac{3N^2 H^4}{32\pi^2} \\ -\frac{3N^2 H^4}{32\pi^2} \\ \frac{\pi^2}{2} N^2 T_0^3 \end{pmatrix}. \quad (2.21)$$

Thus, $\mathcal{N} = 4$ late-time vacuum state in de Sitter is characterized by a cosmological constant, a vanishing local temperature, a constant comoving entropy density, and a vanishing physical entropy density. As a result,

$$\lim_{t \rightarrow \infty} \frac{1}{H^3 a^3} \frac{d}{dt} (a^3 s) = \lim_{t \rightarrow \infty} \left(\frac{1}{H^3 a^3} \times 0 \right) = 0 \quad \implies \quad \mathcal{R}^{\mathcal{N}=4} = 0. \quad (2.22)$$

2.2 Holographic dual perspective

The bulk geometry is characterized by two warp factors A and Σ (2.4). Note that as $t \rightarrow \infty$ (in the $\lambda(t) \equiv 0$ gauge),

$$\lim_{t \rightarrow \infty} A(t, r) \equiv A_v(r) = \frac{r}{8}(r - 8H), \quad \lim_{t \rightarrow \infty} \frac{\Sigma(t, r)}{a(t)} \equiv \sigma_v(r) = \frac{r}{2}. \quad (2.23)$$

One can either use the $t \rightarrow \infty$ limit of (2.11), or compute the location of the AH directly in the "vacuum geometry"

$$ds_{5,vacuum}^2 = 2dt (dr - A_v dt) + e^{2Ht} \sigma_v^2 d\mathbf{x}^2, \quad (2.24)$$

to find

$$r_{AH,vacuum} = 0. \quad (2.25)$$

It is instructive to separate the range of the radial coordinate $r \in [r_{AH,vacuum}, +\infty)$ into two subregions: $r \in [0, 8H] \cup [8H, +\infty)$. Let's consider these subregions separately.

- $r \in [8H, +\infty)$:

In this case $A_v \geq 0$. With the change of coordinates¹¹

$$t \rightarrow \tau + \frac{1}{2H} \ln \left(1 - \frac{8H}{r} \right), \quad (2.26)$$

¹¹This is simply a transformation from the Eddington-Finkelstein to Fefferman-Graham coordinate system.

the vacuum gravitational dual geometry (2.24) takes form

$$ds_{5,vacuum}^2 = \frac{r(r-8H)}{4} \left(-d\tau^2 + e^{2H\tau} d\mathbf{x}^2 \right) + \frac{4dr^2}{r(r-8H)}. \quad (2.27)$$

Further introducing

$$r = 8H \cosh^2 \frac{\rho}{2}, \quad \rho \in [0, +\infty), \quad (2.28)$$

we arrive at

$$ds_{5,vacuum}^2 = 4 \left[H^2 \sinh^2 \rho \left(-d\tau^2 + e^{2H\tau} d\mathbf{x}^2 \right) + d\rho^2 \right], \quad (2.29)$$

which is dS_4 slicing of the Poincare patch AdS_5 geometry [26]. It is easy to see that one gets identical late-time bulk geometry for closed spatial slicing de Sitter boundary (1.1), see [7]. In the latter case,

$$ds_{5,vacuum}^2 = 4 \left[H^2 \sinh^2 \rho \left(-d\tau^2 + \frac{1}{H^2} \cosh^2(H\tau) (dS^3)^2 \right) + d\rho^2 \right], \quad (2.30)$$

which upon analytical continuation $\tau \rightarrow \tau_E = i\theta/H$ becomes

$$ds_{5,vacuum,E}^2 = 4 \left[\sinh^2 \rho (dS^4)^2 + d\rho^2 \right]. \quad (2.31)$$

There can not be any entropy assigned to (2.29)-(2.31). From the periodicity $\theta \sim \theta + 2\pi$ we can formally assign de Sitter temperature (1.5).

- $r \in [0, 8H]$:

Here, $A_v \leq 0$; this part of the geometry is completely invisible from the (Euclidean) de Sitter perspective, as in early studies of the holographic duality of strongly coupled gauge theories in de Sitter background space-time [26–30]. It is “discovered” by asking a dynamical question, *i.e.*, what is the evolution of the holographic gauge theory in de Sitter¹²? The proper bulk coordinates to address this question are the Eddington-Finkelstein ones, and in those coordinates the spatial location with

$$A_v = 0 \quad \implies \quad r = 8H \quad \text{or} \quad \rho = 0, \quad (2.32)$$

is not special; in fact, because of the AH condition (2.11)

$$\text{AH :} \quad 0 = \partial_t \Sigma + A \partial_r \Sigma \quad \underbrace{\simeq}_{t \rightarrow \infty} \quad a(t) (H\sigma_v + A_v \sigma'_v), \quad (2.33)$$

¹²Ref. [31] provides an explicit model of the dynamical evolution.

the spatial location (2.32) is *outside* the AH, and so to reach the AH one needs to extend the geometry for $0 \leq r < 8H$ until the condition (2.33) is satisfied. Working directly in vacuum geometry of the $\mathcal{N} = 4$ SYM (2.24), since

$$\sigma_v \Big|_{r=r_{AH,vacuum}} = 0, \quad (2.34)$$

the physical entropy density of the late-time de Sitter vacuum of the dual $\mathcal{N} = 4$ SYM vanishes¹³ (see (2.12)):

$$s_{ent} = \frac{1}{4G_5} \lim_{t \rightarrow \infty} \left(\frac{\Sigma^3}{a^3} \Big|_{r=r_{AH}} \right) = \frac{1}{4G_5} \sigma_v^3 \Big|_{r=r_{AH,vacuum}} = 0. \quad (2.35)$$

Notice that the surface gravity of the AH is negative

$$\kappa_{vacuum} = A'_v \Big|_{r=r_{AH,vacuum}} = -H. \quad (2.36)$$

2.3 $\mathcal{N} = 4$ SYM de Sitter late-time vacuum

Previously, we obtained the bulk geometry (2.24) dual to late-time de Sitter vacuum of $\mathcal{N} = 4$ SYM plasma by constructing a dual to a dynamical evolution of the thermal state (see (2.4) and (2.10)) and taking the $t \rightarrow \infty$ limit of the latter. The dynamical evolution can be technically quite involved, and is in fact unnecessary if one is interested in the late-time vacuum. Following [7] we introduce

$$\lim_{t \rightarrow \infty} \left\{ A(r, t), \frac{\Sigma(t, r)}{a(t)} \right\} = \{A, \sigma\}_v(r), \quad (2.37)$$

and take the $t \rightarrow \infty$ limit of the equations (2.6)-(2.7) instead

$$0 = \sigma'_v + \frac{\sigma_v}{2A_v}(H - A'_v), \quad 0 = A''_v - 6A_v((\ln \sigma_v)')^2 - 6H(\ln \sigma_v)' + \frac{1}{2}, \quad (2.38)$$

$$0 = \sigma''_v, \quad 0 = \frac{1}{4A_v} - ((\ln \sigma_v)')^2 - \frac{\sigma'_v}{2\sigma_v A_v}(2H + A'_v) + \frac{H}{4A_v^2}(H - A'_v). \quad (2.39)$$

Solution of (2.38)-(2.39) (up to a shift of the radial coordinate) is (2.23).

The first advantage of this approach is the fact that to solve for the dual late-time vacuum geometry one needs to solve the system of ODEs (2.38)-(2.39), instead of PDEs (as in (2.6)-(2.7)), followed by $t \rightarrow \infty$ limit. The second advantage is a

¹³This limit is better defined using the last equality in (2.12).

conceptual one: the late time vacuum state is *universal* while the approach towards it depends on the details of the dynamical evolution of the chosen initial state. Indeed, the thermal state evolution discussed at the beginning of this section depends on a single parameter r_0 , which can be related to the local temperature T_0 of the plasma at $a(t=0) = 1$, see (2.15); alternatively, it defines the constant comoving entropy density during the evolution (as in (2.12)). There is no memory of the r_0 in the energy, pressure or the physical entropy density of the late-time vacuum SYM. Notice that during the evolution of the thermal state, stress energy tensor behaves as

$$T_{\mu\nu}(t) - T_{\mu\nu}^{vacuum} \sim \frac{r_0^4}{a(t)^4} \rightarrow 0 \quad \text{as} \quad t \rightarrow \infty. \quad (2.40)$$

One expects¹⁴ that a more generic homogeneous and isotropic initial state of the $\mathcal{N} = 4$ SYM with initially a non-vanishing expectation value of an operator \mathcal{O} of a fixed scaling dimension Δ

$$\mathcal{O}^\Delta(t=0) = \mathcal{O}_0^\Delta \neq 0, \quad (2.41)$$

would evolve as

$$\mathcal{O}^\Delta(t) \sim \frac{\mathcal{O}_0^\Delta}{a(t)^\Delta} \rightarrow 0 \quad \text{as} \quad t \rightarrow \infty, \quad (2.42)$$

leading to the same late-time vacuum state as the one obtained from the evolution of the thermal state. Notice that in this more general setting the comoving entropy density would increase, saturating at a fixed constant leading to the same conclusion (2.1). This follows from the fact that such more general de Sitter space-time dynamics is Weyl equivalent to a thermalization dynamics in Minkowski space-time (see Appendix B of [7]), in particular, the total comoving entropy produced in de Sitter dynamics is exactly the same as the total entropy produced in corresponding thermalization process of the conformal SYM in Minkowski space-time.

3 $\mathcal{R}_{(m,k)}^{\mathcal{N}=2^*}$

In section 2 we discussed the computation of $\mathcal{R}^{\mathcal{N}=4}$. We begin here outlining the strategy of computing the vacuum comoving entropy production rate \mathcal{R} for $\mathcal{N} = 2^*$ gauge theory for select choices of the mass parameter m (see (1.7)) and the background

¹⁴This is explicitly confirmed by the fact that de Sitter conformal theory vacuum is recovered in the limit of vanishing of the relevant couplings of the non-conformal QFT, see [7, 31] and the analysis of section 3.

space-time curvature coupling constant k (see (1.10)), *i.e.*, $\mathcal{R}_{(m,k)}^{\mathcal{N}=2^*}$. We highlight the differences from the $\mathcal{N} = 4$ SYM case.

- We follow approach of section 2.3 and after deriving the general evolution equations for homogeneous and isotropic state of the $\mathcal{N} = 2^*$ gauge theory in de Sitter (the analogue of (2.6)-(2.7)) we take the late-time limit to arrive at the vacuum equations (the analogue of (2.38) -(2.39)).
- Motivated by the discussion in section 2.2 we consider two subregions of the gravitational bulk geometry: from the asymptotic AdS_5 boundary to $A_v = 0$, and from $A_v = 0$ to the AH specified by (2.33). We use Fefferman-Graham (Schwarzschild) coordinates in the former subregion — this would allow us to make contact with BEFP numerical solution [12]. For the latter subregion we use the Eddington-Finkelstein coordinates. We implement transition between the two coordinate systems at $A_v = 0$.
- The comoving entropy density is computed as in (2.35). Albeit here, contrary to the $\mathcal{N} = 4$ SYM, we find that

$$\sigma_v \Big|_{r=r_{AH,vacuum}} \neq 0, \quad (3.1)$$

provided $m \neq 0$, resulting in nonvanishing $\mathcal{R}_{(m,k)}^{\mathcal{N}=2^*}$.

- We mention in passing (see [7, 31]) that the conformal limit $(m, k) \rightarrow (0, 0)$ is nonanalytic: while σ_v evaluated at the AH horizon vanishes in this limit, it does so with a fractional power of the conformal symmetry breaking scale (*e.g.*, see eq.(3.1) in [31]).
- As in [8], the surface gravity of the AH is universally given by (2.36) for arbitrary (m, k) , see (3.12).

3.1 BEFP and PW effective actions

Effective five-dimensional gravitational action, holographically dual to $\mathcal{N} = 2^*$ gauge theory is¹⁵

$$S_{BEFP} = \frac{1}{16\pi G_5} \int_{\mathcal{M}_5} d^5\xi \sqrt{-g} \left[R - \frac{12}{\eta^2} \partial_\mu \eta \partial^\mu \eta - \frac{4}{(1 - z\bar{z})^2} \partial_\mu z \partial^\mu \bar{z} - V_{BEFP} \right], \quad (3.2)$$

$$V_{BEFP} = -\frac{1}{\eta^4} - 2\eta^2 \frac{1 + z\bar{z}}{1 - z\bar{z}} - \frac{\eta^8}{4} \frac{(z - \bar{z})^2}{(1 - z\bar{z})^2},$$

where

$$z = z_1 - iz_2, \quad \bar{z} = z_1 + iz_2, \quad \eta = e^\alpha. \quad (3.3)$$

The bulk scalars $\{z_i, \alpha\}$ are dual to the operators $\{\mathcal{O}_i, \mathcal{O}_\alpha\}$, implementing the

$$\mathcal{L}_{\mathcal{N}=4} \rightarrow \mathcal{L}_{\mathcal{N}=2^*} \rightarrow \mathcal{L}_{\mathcal{N}=2^*}^{(m,k)}$$

deformations (1.7) and (1.10). Explicitly,

$$\mathcal{O}_\alpha \sim \text{Tr}(|Z_1|^2 + |Z_2|^2), \quad \mathcal{O}_2 \sim \text{Tr}(\chi_1 \chi_1 + \chi_2 \chi_2 + \text{h.c.}), \quad \mathcal{O}_1 \sim \text{Tr}(Z_1^2 + Z_2^2 + \text{h.c.}). \quad (3.4)$$

A consistent truncation

$$z_1 \equiv 0, \quad (3.5)$$

followed by a field redefinition

$$z_2 \equiv \tanh \chi, \quad (3.6)$$

results in PW effective action [9], implementing the deformation (1.7)¹⁶.

We are interested in late-time vacuum states of strongly coupled $\mathcal{N} = 2^*$ gauge theory in de Sitter. The gravity dual ansatz describing dynamical evolution of $SO(4)$ -invariant states is

$$ds_5^2 = 2dt(dr - Adt) + \Sigma^2 (dS^3)^2, \quad (3.7)$$

where the metric warp factors $\{A, \Sigma\}$, and the bulk scalar $\{z_i, \eta\}$, are functions of (t, r) . The equations of motion obtained from (3.2) are given in (A.1)-(A.3). These equations has to be supplemented with the asymptotic $r \rightarrow \infty$ boundary conditions implementing

¹⁵See [18] for the 10d type IIB supergravity uplift.

¹⁶The stability of PW \subset BEFP embedding for the thermal states of $\mathcal{N} = 2^*$ plasma (with $k = 0$) was studied in [32].

the gauge theory background de Sitter space-time (1.1), and the deformation coupling constants (m, k) :

$$\begin{aligned}\Sigma &= \frac{r}{2} \frac{1}{H} \cosh(Ht) + \mathcal{O}(r^0), & A &= \frac{r^2}{8} + \mathcal{O}(r^1), \\ \eta &= 1 - \frac{8m^2 \ln r}{3r^2} + \mathcal{O}(r^{-2}), & z_1 &= \frac{16k \ln r}{r^2} + \mathcal{O}(r^{-2}), & z_2 &= \frac{2m}{r} + \mathcal{O}(r^{-2}).\end{aligned}\tag{3.8}$$

To derive the late-time geometry dual to $\mathcal{N} = 2^*$ vacuum in de Sitter, we introduce following [7]

$$\lim_{t \rightarrow \infty} \left\{ \eta(t, r), z(t, r), \bar{z}(t, r), A(t, r), \frac{H}{\cosh(Ht)} \Sigma(t, r) \right\} = \{ \eta, z, \bar{z}, A, \sigma \}_v(r). \tag{3.9}$$

The full set of the vacuum equations is given in (A.4)-(A.5). The first of the constraint equations in (A.5)

$$0 = \sigma'_v + \frac{\sigma_v}{2A_v} (H - A'_v), \tag{3.10}$$

is very important. Given the location of the AH,

$$AH : \quad (H\sigma_v + A_v\sigma'_v) \Big|_{r=r_{AH, vacuum}} = 0, \tag{3.11}$$

it implies that [8]

$$A'_v \Big|_{r=r_{AH, vacuum}} = -H \quad \implies \quad \kappa_{vacuum} = -H, \tag{3.12}$$

i.e., the surface gravity of the late-time AH is universal — it does not depend on the mass deformation parameters (m, k) .

Generic values of (m, k) completely break the (Euclidean) supersymmetry of the model — as a result the gravitational equations of motion (A.4)-(A.5) are second-order for scalars $\{\eta_v, z_v, \bar{z}_v\}$ (and of the first-order for the metric warp factors $\{A_v, \sigma_v\}$). However, it is straightforward to verify the the following first-order equations¹⁷

$$\begin{aligned}0 &= z'_v + \frac{3\eta'_v(1 - z_v\bar{z}_v)(\eta_v^6(z_v - \bar{z}_v) + 2(z_v + \bar{z}_v))}{2\eta_v(\eta_v^6(\bar{z}_v^2 - 1) + 1 + \bar{z}_v^2)}, \\ 0 &= \bar{z}'_v + \frac{3\eta'_v(1 - z_v\bar{z}_v)(\eta_v^6(\bar{z}_v - z_v) + 2(z_v + \bar{z}_v))}{2\eta_v(\eta_v^6(z_v^2 - 1) + 1 + z_v^2)}, \\ 0 &= (\eta'_v)^2 - \frac{\eta_v^6(z_v^2 - \bar{z}_v^2)^2}{144H^2(1 - z_v\bar{z}_v)^4},\end{aligned}\tag{3.13}$$

¹⁷These equations can be obtained from the BPS eqs. (3.20) and (3.26) of [12] transforming to EF coordinate system and setting $L = 2$.

an algebraic expression for A_v ,

$$A_v = \frac{2H^2(1 - z_v \bar{z}_v)^2(\eta_v^6(z_v^2 - 1) + 1 + z_v^2)(\eta_v^6(\bar{z}_v^2 - 1) + 1 + \bar{z}_v^2)}{\eta_v^8(z_v^2 - \bar{z}_v^2)^2}, \quad (3.14)$$

and σ_v determined from (3.10), solve all the second-order equations (A.4) and the second constraint in (A.5). The BPS-like equations (3.13) constrain the non-normalizable coefficients (m, k) of the scalars $z_{i,v}$ as

$$4k^2 + H^2m^2 = 0, \quad (3.15)$$

which is just a (Euclidean) supersymmetry condition (1.10).

In what follows we set

$$H = 1. \quad (3.16)$$

The correct H -dependence can be recovered from the dimensional analysis.

3.2 $\mathcal{R}_{(m=i\mu, k=\mu H/2)}^{\mathcal{N}=2^*}$ and $\mathcal{R}_{(m=\mu, k=i\mu H/2)}^{\mathcal{N}=2^*}$

Consider first

$$(m, k) = (i\mu, \mu/2), \quad \text{Im } \mu = 0. \quad (3.17)$$

Introduce a new radial coordinate $x \in (0, x^*]$ covering the first bulk subregion (see section 2.2)

$$\frac{dr}{dx} = -\frac{2}{x}(2A_v)^{1/2}, \quad (3.18)$$

implementing the transformation from EF (3.7) to FG coordinate system

$$ds_5^2 = 2A_v \left(-(d\tau)^2 + \frac{1}{H^2} \cosh^2(H\tau)(dS^3)^2 \right) + \frac{4}{x^2} dx^2, \quad d\tau = dt + \frac{2^{1/2}}{x(A_v)^{1/2}} dx, \quad (3.19)$$

where x^* is defined so that

$$A_v \Big|_{x=x^*} = 0. \quad (3.20)$$

Resulting equations¹⁸ for $\{z_v, \bar{z}_v, \eta_v\}$ and s_v , defined as

$$\sigma_v = \frac{1}{x} + s_v, \quad (3.21)$$

are collected in (B.1). They must be solved numerically subject to the following asymptotes:

¹⁸As in [12], the bulk scalars z and \bar{z} should be understood as being independent for “supersymmetric” RG flows.

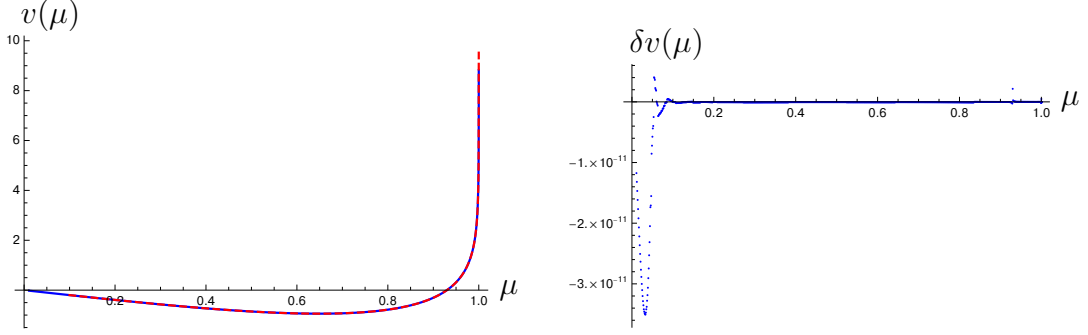


Figure 1: Left panel: numerical values for $v(\mu)$ (see (3.22)) (solid blue curve) and the predicted values $v_{prediction}$ (see (3.25)) (dashed red curve). Right panel: the residual δv (see (3.26)).

- asymptotic AdS boundary, *i.e.*, $x \rightarrow 0_+$,

$$\begin{aligned}
z_v &= \mu x + x^2(-2\mu \ln x + v) + \mathcal{O}(x^3 \ln x), \\
\bar{z}_v &= -\mu x + x^2(-2\mu \ln x + v) + \mathcal{O}(x^3 \ln x), \\
\eta_v &= 1 - \frac{\mu}{3}(2\mu \ln x - \mu - v)x^2 + \mathcal{O}(x^4), \quad s_v = 2 + x \left(1 + \frac{\mu^2}{3}\right) + \mathcal{O}(x^2),
\end{aligned} \tag{3.22}$$

where $v = v(\mu)$ is a single UV parameter;

- $A_v = 0$, *i.e.*, $y \equiv (x^* - x) \rightarrow 0_+$,

$$\begin{aligned}
z_v &= \sqrt{\frac{e_0^6 - 1}{e_0^6 + 1}} \left(1 - \frac{e_0^2}{3(x^*)^2} y^2 + \mathcal{O}(y^3)\right), \\
\bar{z}_v &= \sqrt{\frac{e_0^6 - 1}{e_0^6 + 1}} \left(\frac{e_0^6 - 2}{e_0^6 + 2} - \frac{e_0^2(11e_0^{12} - 20)}{15(x^*)^2(e_0^6 + 2)^2} y^2 + \mathcal{O}(y^3)\right), \\
\eta_v &= e_0 - \frac{e_0^{12} - 1}{27e_0^3(x^*)^2} y^2 + \mathcal{O}(y^3), \quad s_v = s_0 - \frac{1}{(x^*)^2} y + \mathcal{O}(y^2),
\end{aligned} \tag{3.23}$$

characterized 3 additional parameters $\{e_0, s_0, x^*\}$. Note that

$$2A_v = \frac{4}{(x^*)^2} y^2 + \frac{4}{(x^*)^3} y^3 + \frac{28e_0^{12} + 297e_0^4 + 80}{81e_0^4(x^*)^4} y^4 + \mathcal{O}(y^5), \tag{3.24}$$

thus, both the bulk geometry and the scalars are smooth in the vicinity of x^* .

Holographic renormalization of the model, along with the result for the free energy computed from the localization [14], makes a specific prediction for $v(\mu)$ [12]:

$$v \Big|_{prediction} = -2\mu - \mu \ln(1 - \mu^2). \quad (3.25)$$

Using the shooting method developed in [33], we recover numerical results of [12], and confirm the prediction (3.25): fig. 1 shows $v(\mu)$ (left panel, solid blue curve) and $v_{prediction}$ (left panel, dashed red curve) and the residual δv (right panel)

$$\delta v \equiv 1 - \frac{v(\mu)}{v_{prediction}}. \quad (3.26)$$

To compute the comoving entropy production rate $\mathcal{R}_{(m=i\mu, k=\mu H/2)}^{\mathcal{N}=2^*}$ we need an access to the second subregion of the bulk geometry with $A_v \leq 0$, see discussion in section 2.2. This is done returning to the original ER coordinate r , see (3.18). Introduce

$$r = r^* - \rho, \quad \rho \in [0, \rho_{AH}] \iff r \in [r_{AH, vacuum}, r^*], \quad (3.27)$$

where

$$r^* = r \Big|_{x=x^*}. \quad (3.28)$$

The holographic equations of motion in ρ coordinate are simply (3.13) with

$$\partial_r \equiv ' = -\partial_\rho.$$

For small $\rho < 0$ we obtain from the perturbative integration of (3.18)

$$-\rho = \frac{2}{(x^*)^2} y^2 + \frac{2}{(x^*)^3} y^3 + \frac{(7e_0^{12} + 297e_0^4 + 20)}{162e_0^4(x^*)^4} y^4 + \mathcal{O}(y^5), \quad (3.29)$$

or

$$y = \frac{(-\rho)^{1/2} x^*}{2^{1/2}} \left(1 - \frac{1}{2^{3/2}} (-\rho)^{1/2} - \frac{7e_0^{12} - 108e_0^4 + 20}{1296e_0^4} (-\rho) + \frac{2^{1/2}(7e_0^{12} - 27e_0^4 + 20)}{2592e_0^4} (-\rho)^{3/2} + \mathcal{O}((-\rho)^2) \right), \quad (3.30)$$

which is used to set up the asymptotic initial conditions from (3.23)

$$\begin{aligned}
z_v &= \sqrt{\frac{e_0^6 - 1}{e_0^6 + 1}} \left(1 + \frac{1}{6} e_0^2 \rho + \frac{16e_0^{12} + 45e_0^6 + 20}{3240e_0^2} \rho^2 + \mathcal{O}(\rho^3) \right), \\
\bar{z}_v &= \sqrt{\frac{e_0^6 - 1}{e_0^6 + 1}} \left(\frac{e_0^6 - 2}{e_0^6 + 2} + \frac{e_0^2(11e_0^{12} - 20)}{30(e_0^6 + 2)^2} \rho \right. \\
&\quad \left. + \frac{1304e_0^{30} + 10231e_0^{24} + 8750e_0^{18} - 10220e_0^{12} - 15400e_0^6 - 5600}{113400e_0^2(e_0^6 + 2)^3} \rho^2 + \mathcal{O}(\rho^3) \right), \\
\eta_v &= e_0 + \frac{e_0^{12} - 1}{54e_0^3} \rho + \frac{11e_0^{24} - e_0^{12} - 10}{6480e_0^7} \rho^2 + \mathcal{O}(\rho^3), \\
\sigma_v &= \frac{s_0 x^* + 1}{x^*} - \frac{7e_0^{12} s_0 x^* + 7e_0^{12} + 20s_0 x^* + 20}{216x^* e_0^4} \rho \\
&\quad - \frac{53e_0^{24} s_0 x^* + 53e_0^{24} - 133e_0^{12} s_0 x^* - 133e_0^{12} + 80s_0 x^* + 80}{29160e_0^8 x^*} \rho^2 + \mathcal{O}(\rho^3).
\end{aligned} \tag{3.31}$$

Note that

$$A_v = -\rho + \frac{7e_0^{12} + 20}{216e_0^4} \rho^2 + \frac{53e_0^{24} - 133e_0^{12} + 80}{21870e_0^8} \rho^3 + \mathcal{O}(\rho^4). \tag{3.32}$$

Combining (3.10) and (3.11) we have

$$\frac{\sigma_v}{2} (H + A'_v) = \frac{H(\eta_v^6(z_v^2 - 1) - 2(z_v^2 + 1))(\eta_v^6(\bar{z}_v^2 - 1) + \bar{z}_v^2 + 1)\sigma_v}{6\eta_v^2(z_v^2 - \bar{z}_v^2)} \Big|_{r=r_{AH,vacuum}} = 0, \tag{3.33}$$

where in the second equality we used explicit expression for A_v (3.14) and the RG flow equations (3.13). Eq. (3.33) motivates introduction of the AH-monitoring function

$$Z_{AH} \equiv \frac{(\eta_v^6(z_v^2 - 1) - 2(z_v^2 + 1))(\eta_v^6(\bar{z}_v^2 - 1) + \bar{z}_v^2 + 1)}{6\eta_v^2(z_v^2 - \bar{z}_v^2)}, \quad Z_{AH} \Big|_{\rho=\rho_{AH}} = 0. \tag{3.34}$$

Interestingly, from (3.31)

$$Z_{AH} = 1 - \frac{7e_0^{12} + 20}{216e_0^4} \rho - \frac{53e_0^{24} - 133e_0^{12} + 80}{14580e_0^8} \rho^2 + \mathcal{O}(\rho^3), \tag{3.35}$$

independent of μ .

Typical profiles of the metric warp factors $\{A_v, \sigma_v\}$ (solid black and blue curves, left panel), the bulk scalars $\{z_v, \bar{z}_v, \eta_v\}$ (solid blue, magenta and black curves, right

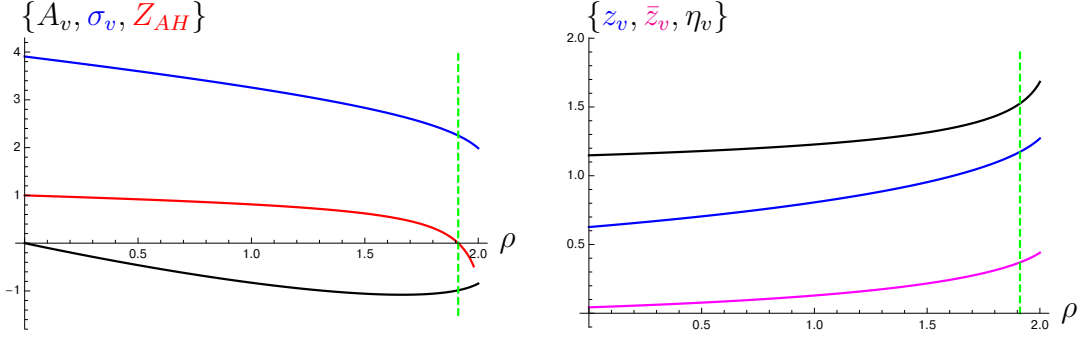


Figure 2: We set $\mu = 0.9$. Left panel: profiles for $\{A_v, \sigma_v, Z_{AH}\}$. Right panel: profiles for $\{z_v, \bar{z}_v, \eta_v\}$. The vertical dashed green line indicates the location of the apparent horizon. The radial coordinate $\rho \in [0, \rho_{AH}+)$ (2.28) covers the second gravitational bulk subregion (see discussion in section 2.2).

panel), and the AH monitoring function Z_{AH} (solid red curve, left panel) are presented in fig. 2 for $\mu = 0.9$. The vertical dashed green line indicates the location of the AH,

$$\rho_{AH} \Big|_{\mu=0.9} = 1.9117(4). \quad (3.36)$$

Most importantly, contrary to the $\mathcal{N} = 4$ SYM (2.34), we find here

$$\sigma_v \Big|_{\rho=\rho_{AH}(\mu=0.9)} = 2.2519(7) \neq 0, \quad (3.37)$$

resulting in

$$\begin{aligned} \mathcal{R}_{(i\mu, \mu H/2)}^{\mathcal{N}=2^*} &= \frac{1}{H^3} s_{ent} = \frac{1}{4G_5} \sigma_v^3 \Big|_{\rho=\rho_{AH}} = \frac{N^2}{16\pi} \sigma_v^3 \Big|_{\rho=\rho_{AH}} \implies \\ \frac{16\pi}{N^2} \mathcal{R}_{(i\mu, \mu H/2)}^{\mathcal{N}=2^*} \Big|_{\mu=0.9} &= 11.420(6). \end{aligned} \quad (3.38)$$

We collect \mathcal{R} results for different values of μ at the end of this section.

We now outline the differences in the second example considered

$$(m, k) = (\mu, i\mu/2), \quad \text{Im} \mu = 0. \quad (3.39)$$

All the analysis proceed literally unchanged once we introduce

$$z_v = i \hat{z}_v, \quad \bar{z}_v = i \hat{\bar{z}}_v, \quad (3.40)$$

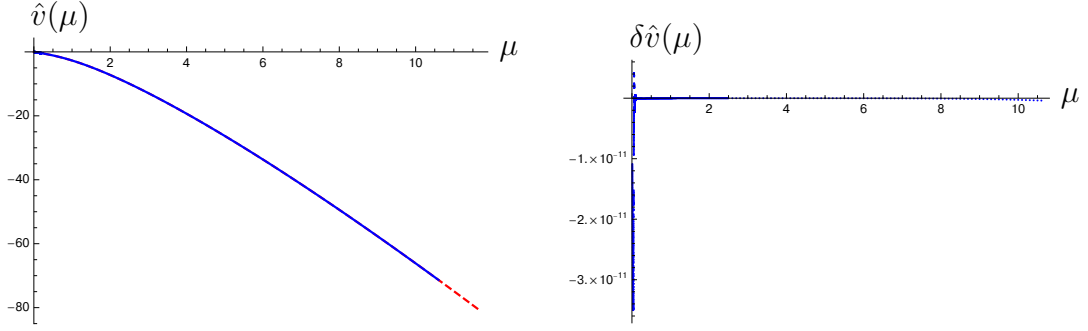


Figure 3: Left panel: numerical values for $\hat{v}(\mu)$ (see (3.41)) (solid blue curve) and the predicted values $\hat{v}_{prediction}$ (see (3.42)) (dashed red curve). Right panel: the residual $\delta\hat{v}$ (see (3.43)).

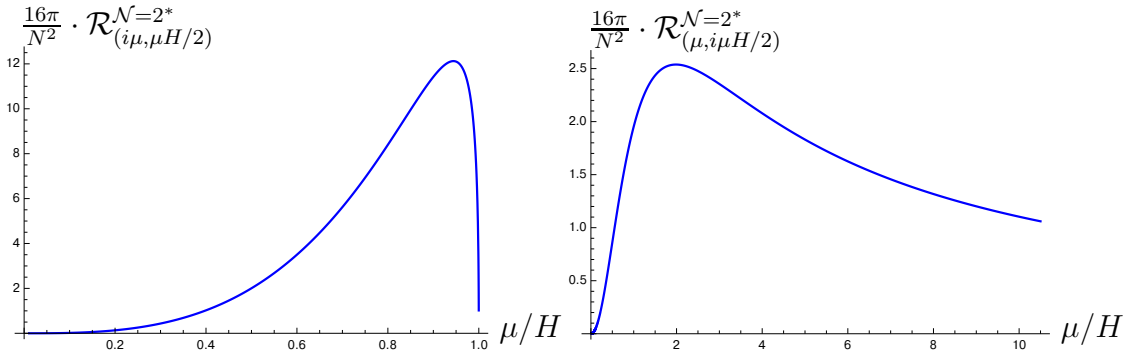


Figure 4: $\mathcal{R}_{(m=i\mu, k=\mu H/2)}^{\mathcal{N}=2^*}$ (left panel) and $\mathcal{R}_{(m=\mu, k=i\mu H/2)}^{\mathcal{N}=2^*}$ (right panel) as a function of μ/H .

so that (3.22) is modified to

$$\begin{aligned}\hat{z}_v &= -\mu x + x^2(2\mu \ln x - \hat{v}) + \mathcal{O}(x^3 \ln x), \\ \hat{\hat{z}}_v &= \mu x + x^2(2\mu \ln x - \hat{v}) + \mathcal{O}(x^3 \ln x).\end{aligned}\tag{3.41}$$

Eq. (3.25) now reads

$$\hat{v} \Big|_{prediction} = -2\mu - \mu \ln(1 + \mu^2).\tag{3.42}$$

Numerical results for $\hat{v}(\mu)$ and the residual $\delta\hat{v}$

$$\delta\hat{v} = 1 - \frac{\hat{v}(\mu)}{\hat{v}_{prediction}},\tag{3.43}$$

are collected in fig. 3.

Fig. 4 is the main result of the section. It shows $\mathcal{R}_{(m=i\mu, k=\mu H/2)}^{\mathcal{N}=2^*}$ (left panel) and $\mathcal{R}_{(m=\mu, k=i\mu H/2)}^{\mathcal{N}=2^*}$ (right panel) as a function of μ/H . Unlike (3.25) and (3.42), we have been unable to guess the analytic expressions for \mathcal{R} . As we already stated in section 1, the challenge for the localization is to reproduce the predictions reported here.

3.3 $\mathcal{R}_{(m=\mu, k=\mu H/2)}^{\mathcal{N}=2^*}$

With

$$(m, k) = (\mu, \mu/2), \quad \text{Im} \mu = 0, \quad (3.44)$$

there is no (Euclidean) supersymmetry, and the holographic RG flows are of the second order, see (A.4) and (A.5). We discuss this case in some details, as the techniques developed are vital for understanding de Sitter vacua of cascading gauge theories [21].

We use a new radial coordinate $x \in (0, \infty)$ covering the first bulk subregion (see section 2.2)

$$r = \frac{H}{x}, \quad (3.45)$$

implementing the transformation from EF (3.7) to FG coordinate system

$$\begin{aligned} ds_5^2 &= \frac{H^2}{x^2 h^{1/2}(x)} \left(-(d\tau)^2 + \frac{1}{H^2} \cosh^2(H\tau) (dS^3)^2 \right) + \frac{h^{1/2}(x)}{x^2} dx^2, \\ d\tau &= dt + \frac{h^{1/2}(x)}{H} dx, \end{aligned} \quad (3.46)$$

where we impose

$$\lim_{x \rightarrow \infty} x^2 h(x) = \frac{1}{4}, \quad (3.47)$$

which ensures that the geometry (3.46) is smooth in the limit $y \equiv \frac{1}{x} \rightarrow 0$

$$\begin{aligned} ds_5^2 &\sim \left(\sqrt{2y} \right)^2 \left(-(Hd\tau)^2 + \cosh^2(H\tau) (dS^3)^2 \right) + \left(d\sqrt{2y} \right)^2 + \mathcal{O}(y^2), \\ ds_{5,E}^2 &\underset{\tau \rightarrow \tau_E = i\theta/H}{\sim} \left(\sqrt{2y} \right)^2 (dS^4)^2 + \left(d\sqrt{2y} \right)^2 + \mathcal{O}(y^2). \end{aligned} \quad (3.48)$$

The full set of the vacuum equations of motion obtained from (A.4) and (A.5) is collected in appendix C. Note that we introduced

$$\sigma(x) = \frac{Hs(x)}{xh^{1/4}(x)}, \quad s(y \equiv \frac{1}{x}) = \frac{\hat{s}(y)}{y^{1/2}}. \quad (3.49)$$

Equations (C.1) must be solved numerically subject to the following asymptotes:

- asymptotic AdS boundary, *i.e.*, $x \rightarrow 0_+$,

$$\begin{aligned}
z_{1,v} &= x^2 (z_{1,2,0} + 8\mu\kappa \ln x) + \mathcal{O}(x^3 \ln x), \\
z_{2,v} &= 2\mu x + \frac{\mu h_1}{32} x^2 + x^3 \left(z_{2,3,0} + \left(\frac{32}{3} \mu^3 + 32\mu \right) \ln x \right) + \mathcal{O}(x^4 \ln x), \\
\eta_v &= 1 + x^2 \left(e_{2,0} + \frac{8}{3} \mu^2 \ln x \right) + \mathcal{O}(x^3 \ln x), \\
h &= 16 + h_1 x + \mathcal{O}(x^2), \quad s = 1 + 4x + \mathcal{O}(x^2),
\end{aligned} \tag{3.50}$$

where we showed explicitly the dependence on normalizable coefficients $\{z_{1,2,0}, z_{2,3,0}, h_1, e_{2,0}\}$; the parameter¹⁹ $\kappa = \{\pm 1, 0\}$ corresponding to $k = \kappa\mu/2$;

- $h \rightarrow 0$, *i.e.*, $y \equiv \frac{1}{x} \rightarrow 0_+$,

$$\begin{aligned}
z_{1,v} &= z_{1,0}^h + \mathcal{O}(y), & z_{2,v} &= z_{2,0}^h + \mathcal{O}(y), & \eta_v &= \eta_0^h + \mathcal{O}(y), \\
h &= \frac{1}{4} y^2 + \mathcal{O}(y^3), & \hat{s} &= s_0^h + \mathcal{O}(y).
\end{aligned} \tag{3.51}$$

Notice that fixing $\{\mu, \kappa\}$, the holographic RG flows are completely determined by 8 parameters

$$\{z_{1,2,0}, z_{2,3,0}, h_1, e_{2,0}\} \cup \{z_{1,0}^h, z_{2,0}^h, \eta_0^h, s_0^h\}, \tag{3.52}$$

which is the correct overall number to specify a solution for a system (C.1) of 3 second-order differential equations and 2 first-order differential equations. This has to be contrasted with the (Euclidean) supersymmetric flows (B.1), which are determined by 4 parameters: $\{v, x^*, e_0, s_0\}$ (see (3.22) and (3.23)). Of course, these supersymmetric flows represent a special case of the RG flows discussed in this section: after relating the radial coordinates, the UV parameters (3.50) and (3.22) are matched as follows

Eq. (3.50)	Eq. (3.22)
μ	$i\mu$
$z_{1,2,0}$	$4v - 8\mu \ln 2$
$iz_{2,3,0}$	$\left(\frac{32}{3} \ln 2 - 8\right) \mu^3 - \frac{16}{3} \mu^2 v - \left(\frac{h_1^2}{2048} + 32 \ln 2\right) \mu + 16v$
$e_{2,0}$	$\frac{4}{3} v \mu + \left(\frac{4}{3} - \frac{8}{3} \ln 2\right) \mu^2$

¹⁹There is an exact \mathbb{Z}_2 symmetry $z_{1,v} \leftrightarrow -z_{1,v}$ implying that the choice of a sign of κ is physically irrelevant.

Parameter h_1 remains unfixed in UV; this is related to the residual symmetry of the metric ansatz (3.45)

$$x \rightarrow \frac{x}{1 + \alpha x}, \quad h \rightarrow (1 + \alpha x)^4 h, \quad \alpha = \text{const.} \quad (3.53)$$

This symmetry is fixed with the boundary condition in IR, see (3.47).

We use the numerical shooting method adopted from [30] to construct RG flows for various values of μ and $\kappa = \{1, 0\}$ realizing the first subregion of the dual geometry as per discussion in section 2.2. To compute the comoving entropy production rate $\mathcal{R}_{(\mu, \kappa \mu/2)}^{\mathcal{N}=2^*}$ we need an access to the second subregion of the bulk geometry with $A_v \leq 0$. This is done returning to the original ER coordinate r , see (3.18). Introduce

$$r = -\rho \equiv y, \quad \rho \in [0, \rho_{AH}] \iff r \in [r_{AH, \text{vacuum}}, 0]. \quad (3.54)$$

The holographic equations of motion in ρ coordinate are simply (A.4) with

$$\partial_r \equiv ' = -\partial_\rho.$$

Given (3.51) and the identification $\rho \equiv -y$, it is trivial to provide asymptotic initial conditions for (A.4) (eqs. (A.5) are satisfied as well, but we will not use them)

$$\begin{aligned} A_v &\equiv \frac{y^2}{2h^{1/2}(y)} \Big|_{y=-\rho} = -\rho - \frac{1}{24} \left(\frac{(\eta_0^h)^8 (z_{2,0}^h)^2}{((z_{1,0}^h)^2 + (z_{2,0}^h)^2 - 1)^2} + \frac{2((z_{1,0}^h)^2 + (z_{2,0}^h)^2 + 1)(\eta_0^h)^2}{(z_{1,0}^h)^2 + (z_{2,0}^h)^2 - 1} \right. \\ &\quad \left. - \frac{1}{(\eta_0^h)^4} \right) \rho^2 + \mathcal{O}(\rho^3), \\ \sigma_v &= \frac{y^{1/2} \hat{s}(y)}{h^{1/4}(y)} \Big|_{y=-\rho} = s_0^h \sqrt{2} \left(1 + \frac{1}{24} \left(\frac{(\eta_0^h)^8 (z_{2,0}^h)^2}{((z_{1,0}^h)^2 + (z_{2,0}^h)^2 - 1)^2} \right. \right. \\ &\quad \left. \left. + \frac{2((z_{1,0}^h)^2 + (z_{2,0}^h)^2 + 1)(\eta_0^h)^2}{(z_{1,0}^h)^2 + (z_{2,0}^h)^2 - 1} - \frac{1}{(\eta_0^h)^4} \right) \rho \right) + \mathcal{O}(\rho^2), \\ z_{1,v} &= z_{1,0}^h + \frac{z_{1,0}^h (\eta_0^h)^2}{10} \left(\frac{(\eta_0^h)^6 (z_{2,0}^h)^2}{(z_{1,0}^h)^2 + (z_{2,0}^h)^2 - 1} + 2 \right) \rho + \mathcal{O}(\rho^2), \\ z_{2,v} &= z_{2,0}^h - \frac{z_{2,0}^h (\eta_0^h)^2}{20} \left(\frac{(\eta_0^h)^6 ((z_{1,0}^h)^2 - (z_{2,0}^h)^2 - 1)}{(z_{1,0}^h)^2 + (z_{2,0}^h)^2 - 1} - 4 \right) \rho + \mathcal{O}(\rho^2), \\ \eta_v &= \eta_0^h - \frac{1}{30} \left(\frac{2(\eta_0^h)^9 (z_{2,0}^h)^2}{((z_{1,0}^h)^2 + (z_{2,0}^h)^2 - 1)^2} + \frac{((z_{1,0}^h)^2 + (z_{2,0}^h)^2 + 1)(\eta_0^h)^3}{(z_{1,0}^h)^2 + (z_{2,0}^h)^2 - 1} + \frac{1}{(\eta_0^h)^3} \right) \rho + \mathcal{O}(\rho^2). \end{aligned} \quad (3.55)$$

AH-monitoring function here is

$$Z_{AH} \equiv \sigma_v - A_v \frac{d\sigma_v}{d\rho}, \quad Z_{AH} \Big|_{\rho=\rho_{AH}} = 0. \quad (3.56)$$

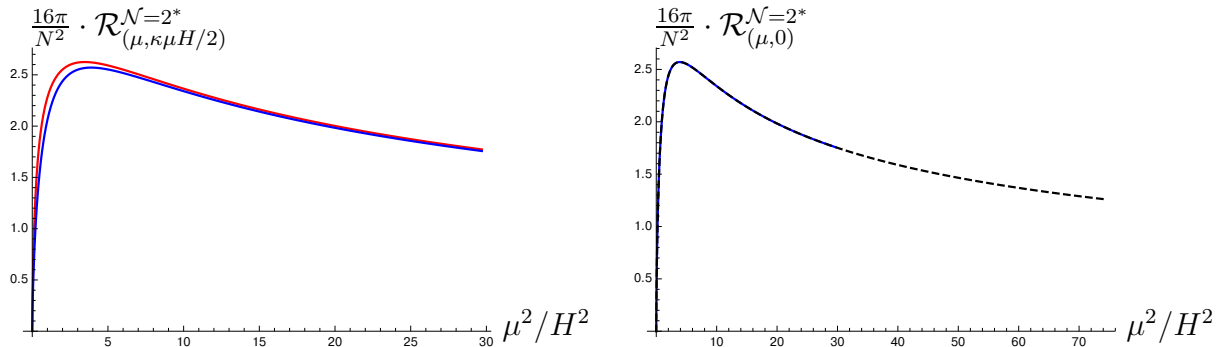


Figure 5: $\mathcal{R}_{(m=\mu, k=\kappa\mu H/2)}^{\mathcal{N}=2^*}$ for $\kappa = 1$ and $\kappa = 0$ (left panel) as a function of μ^2/H^2 . Right panel shows comparison of the results for $\mathcal{R}_{m=\mu, k=0}^{\mathcal{N}=2^*}$ obtained using the method discussed here (solid blue curve) and the equivalent results obtained in [7] (dashed black curve).

Fig. 5 is the main result of the section. It shows $\mathcal{R}_{(m=\mu, k=\kappa\mu H/2)}^{\mathcal{N}=2^*}$ for $k = \{1, 0\}$ (left panel, {red, blue} curves). The effect of the curvature coupling k is relatively small and decreases as μ get larger — this is easy to understand, given that $\frac{k}{\mu^2} \sim \frac{H}{\mu} \rightarrow 0$ as $\frac{\mu^2}{H^2} \rightarrow \infty$. Recall that the computations in this section were performed splitting the holographic geometry into two subregions (see discussion in section 2.2): from the asymptotic AdS boundary to $A_v = 0$ (the first subregion) and from $A_v = 0$ to the apparent horizon (the second subregion). We used Fefferman-Graham (Schwarzschild) coordinates in the first subregion and Eddington-Finkelstein coordinates in the second subregion. The transition between the two coordinate systems was implemented at $A_v = 0$. On the contrary, the computations of $\mathcal{R}_{m=\mu, k=0}^{\mathcal{N}=2^*}$ in [7] were performed entirely in Eddington-Finkelstein coordinate system. Comparison of the two approaches is shown in right panel, fig. 5: blue solid curve is the new result, dashed black curve represent results obtained in [7]. The agreement is $\sim 10^{-4}$ for $\mu < H$ and $\sim 10^{-6}$ (and rapidly improving) for $\mu > H$. This validates the computational method for the comoving entropy production rate \mathcal{R} developed here.

4 Discussion

This paper is a continuation of the exploration of de Sitter vacua of non-conformal gauge theories initiated in [7].

Thermal equilibrium states of interacting QFTs in Minkowski space-time are (typi-

cally²⁰) universal end-points of late-time dynamical evolution. Likewise, de Sitter vacua of interactive QFTs are also universal end-points of late-time dynamical evolution [7]. However, these vacua are definitely not the equilibrium states. There are simple ways to see this:

- first, it is inconsistent to recast late-time evolution in de Sitter as hydrodynamics — the “local temperature” dilutes with the metric scale factor as e^{-Ht} , while the typical velocity gradients remain constant $|\partial u| \sim H$, and thus the standard hydrodynamic approximation, *i.e.*, $|\partial u|/T_{loc} \ll 1$ is not valid;
- second, there is no comoving entropy production in equilibrium states; here, unless the quantum field theory is conformal, there is non-vanishing comoving entropy production rate \mathcal{R} at late time $Ht \gg 1$.

The comoving entropy production rate \mathcal{R} in de Sitter vacuum implies that there is a nonzero vacuum entropy density

$$s_{ent} = H^3 \mathcal{R}. \quad (4.1)$$

The latter quantity is renormalization scheme independent, and might serve as a valuable tool to classify symmetry breaking phases of the theories in de Sitter²¹.

In this paper we expended the computations of \mathcal{R} in $\mathcal{N} = 2^*$ gauge theory in [7], including the curvature coupling k (see (1.10)). We showed that unless both $\mu = 0$ and $k = 0$ (see fig. 6 for results for $\mathcal{R}_{(m=0, k=\mu H/2)}^{\mathcal{N}=2^*}$; this is a special case of the general approach considered in section 3.3) the comoving entropy production rate is non-zero. We developed a new approach towards computation of \mathcal{R} : the dual gravitational geometry is split into two subregions — from the asymptotic *AdS* boundary to $g_{tt} = 0$, and from $g_{tt} = 0$ to the apparent horizon — with Fefferman-Graham (Schwarzschild) coordinates used in the first subregion, and the Eddington-Finkelstein coordinates used in the second subregion. The transition between the two subregions is implemented at $g_{tt} = 0$. This approach differs from the one employed in [7], where the Eddington-Finkelstein coordinates covered the whole bulk geometry. We showed that both methods produce identical results, whenever appropriate. The advantage of the newly proposed method is that it allows the computation of \mathcal{R} in the theories where it is difficult (impossible?) to define the asymptotic Eddington-Finkelstein coordinates (as it is in the case of cascading gauge theories [21]).

²⁰There are exceptions [34].

²¹We discuss this in forthcoming publication.

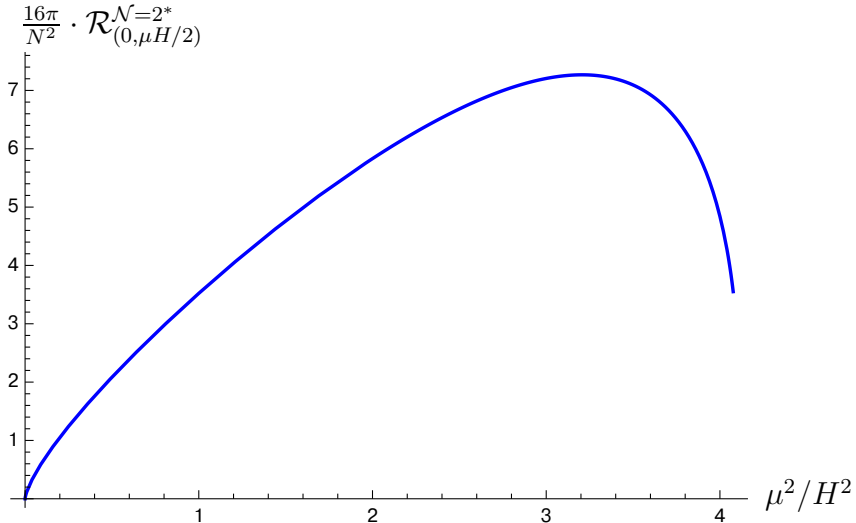


Figure 6: $\mathcal{R}_{(m=0,k=\mu H/2)}^{\mathcal{N}=2^*}$ as a function of μ^2/H^2 . Here, the conformal symmetry is broken by the nonvanishing coupling k to the background space-time, see (1.10). The profile for the comoving entropy production rate is similar to the one in $\mathcal{N} = 2^*$ gauge theory with $k = 0$, and different masses for the bosonic $m_b \neq 0$ and fermionic $m_f = 0$ components in $\mathcal{N} = 2$ hypermultiplet, see left panel of fig. 8 in [7].

For generic values of (m, k) there is no supersymmetry. However, when

$$k = \pm i \frac{Hm}{2}, \quad (4.2)$$

the holographic RG flow equations are of the first order. The BPS-like character of the flow equations reflects the fact that the Wick rotation $H\tau \rightarrow i\theta$ of the first bulk subregion (3.19) represents supersymmetric holographic dual to $\mathcal{N} = 2^*$ gauge theory on S^4 [12, 13, 18]. Powerful techniques of supersymmetric localization exist to compute plethora of properties of strongly coupled $\mathcal{N} = 2^*$ gauge theory without resorting to holography [13–17, 19]. We computed $\mathcal{R}_{(m,k=imH/2)}^{\mathcal{N}=2^*}$ in section 3.2. We hope that the supersymmetric localization of [13] will ultimately shed light on this quantity and its physical origin.

We conclude with our two failed attempts to interpret s_{ent} .

4.1 s_{ent} as a thermal entropy of pair-produced particles

In a dynamical expanding Universe a minimally coupled free massless scalar field experiences particle production. While particle pair production in different momentum

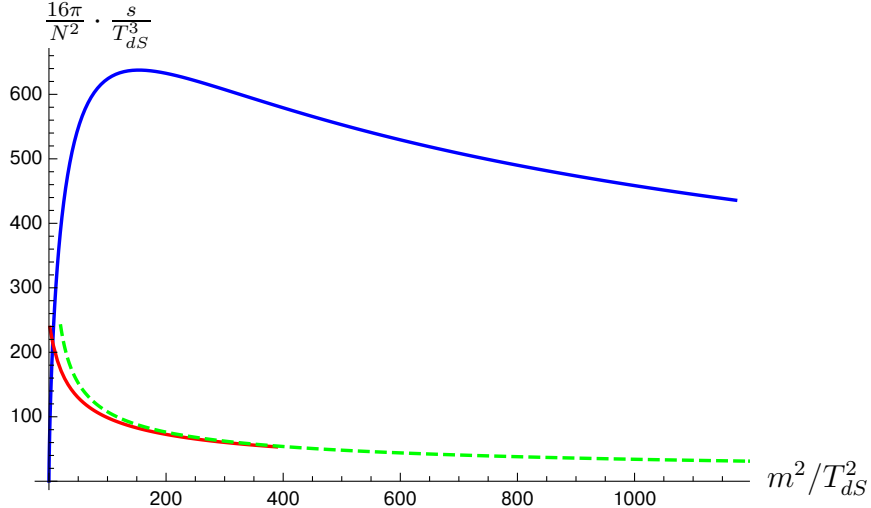


Figure 7: de Sitter vacuum entanglement entropy density s_{ent} of $\mathcal{N} = 2^*$ gauge theory at $(m \neq 0, k = 0)$ (solid blue curve) and the thermal entropy density of the theory $s_{thermal}$ as a function of m^2/T^2 with $T = T_{dS} = H/(2\pi)$. Green dashed curve is the analytic asymptote of $s_{thermal}$ as $m^2/T^2 \rightarrow \infty$, see (4.4).

modes are independent events, pairs produced in a given mode correlate. Local observers will be unable to detect the correlations for produced pairs separated by cosmological scales. As a result, the observed spectrum of produced particles is thermal²².

For an interactive quantum field theory in de Sitter space-time one expects that the pair production will be incoherent at late times, leading to a thermal spectrum with de Sitter temperature T_{dS} (1.5) (see also [36]). Thus, it is tempting to identify

$$s_{ent} = s_{thermal} \Big|_{T=T_{dS}=\frac{H}{2\pi}}. \quad (4.3)$$

Unfortunately, the identification (4.3) can not be correct:

- it is incorrect for conformal field theories, where $s_{ent}^{CFT} \propto \mathcal{R}^{CFT} = 0$, while $s_{thermal}^{CFT} \propto H^3$;
- as fig. 7 shows, it is also incorrect for $\mathcal{N} = 2^*$ gauge theory.

Fig. 7 presents results for the entanglement entropy s_{ent} for $\mathcal{N} = 2^*$ gauge theory with $(m \neq 0, k = 0)$ as a function of m^2/T_{dS}^2 (the solid blue curve), and the thermodynamic entropy of the theory at equivalent value $T = T_{dS}$ (the solid red curve). The dashed green curve represents the asymptotic of the thermodynamic entropy as

²²See [35] for a nice presentation.

$m^2 \gg T_{dS}^2$,

$$\frac{16\pi}{N^2} \cdot \frac{s_{thermal}}{T_{dS}^3} \sim \frac{6912\pi^4}{625} \left(\frac{m^2}{T_{dS}^2} \right)^{-1/2}, \quad (4.4)$$

computed in appendix D. Note that

$$\frac{16\pi}{N^2} \cdot \frac{s_{thermal}}{T_{dS}^3} \Big|_{m^2/T_{dS}^2 \rightarrow 0} = 8\pi^3. \quad (4.5)$$

From fig. 7 it is clear that there is no obvious relation between s_{ent} and a "subtracted" thermodynamic entropy

$$\frac{s_{subtracted}}{T^3} \equiv \frac{s_{thermal}}{T^3} \Big|_{T=T_{dS}} - \frac{s_{thermal}}{T^3} \Big|_{T \rightarrow \infty} \quad (4.6)$$

— at the very least, by definition, $s_{subtracted}$ vanishes for CFTs.

4.2 s_{ent} as a thermodynamic entropy of the localization free energy at $T = T_{dS}$

In holographic thermodynamics, the thermal free energy density $f_{thermal}$ is related to the renormalized Euclidean bulk gravitational action \mathcal{I}_E as follows

$$\mathcal{I}_E = \underbrace{\int_{\mathcal{M}_3} d^3x \int dt_E}_{\int_{\mathcal{M}_4^E} d\xi^4} f_{thermal}, \quad (4.7)$$

where $\int_{\mathcal{M}_3} d^3x$ is the spatial integral, and $\int dt_E = \frac{1}{T}$ is the integral over the (compactified) Euclidean temporal direction. We denoted $\int_{\mathcal{M}_4^E} d\xi^4$ as the integral over the Euclidean space-time. From (4.7), the average free energy density

$$\langle f_{thermal} \rangle = \frac{1}{\text{vol}\mathcal{M}_4^E} \mathcal{I}_E. \quad (4.8)$$

We would like to apply (4.8) to $\mathcal{I}_E = \mathcal{F}$, with \mathcal{F} computed either via supersymmetric localization [14] or in holography [12] (up to scheme dependence, both computations agree). Using

$$\text{vol}\mathcal{M}_4^E = \frac{8}{3}\pi^2 \ell_{S^4}^4 = \frac{8\pi^2}{3H^4}, \quad (4.9)$$

where the radius of S^4 is $\ell_{S^4} = 1/H$, we find

$$\frac{16\pi}{N^2} \langle f_{thermal} \rangle = -\frac{3H^4}{\pi} \left(\left(1 + \frac{m^2}{H^2} \right) \ln \left(1 + \frac{m^2}{H^2} \right) + \alpha_0 + \alpha_1 \frac{m}{H} + \alpha_2 \frac{m^2}{H^2} \right); \quad (4.10)$$

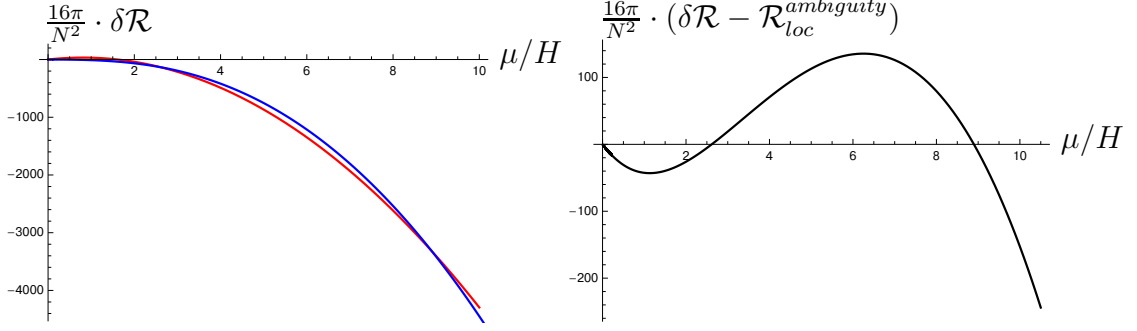


Figure 8: Left panel: comparison of $\delta\mathcal{R} = \mathcal{R}_{(\mu, i\mu H/2)}^{\mathcal{N}=2^*} - \mathcal{R}_{loc}^0$ (blue curve) and the best two parameter fit $\delta\mathcal{R} = \mathcal{R}_{loc}^{ambiguity}$ (red curve). Right panel: the residual $\delta\mathcal{R} - \mathcal{R}_{loc}^{ambiguity}$ (black curve).

the arbitrary coefficients α_i parameterize the *full* renormalization scheme dependence [20]. Applying the first law of thermodynamics to $\langle f_{thermal} \rangle$ with $H = 2\pi T_{dS}$, we identify

$$s_{ent,loc} = -\frac{d\langle f_{thermal} \rangle}{dT_{dS}}, \quad (4.11)$$

leading to (see (1.4))

$$\begin{aligned} \frac{16\pi}{N^2} \cdot \mathcal{R}_{loc} &\equiv \frac{16\pi}{N^2} \cdot \frac{s_{ent,loc}}{(2\pi T_{dS})^3} \equiv \frac{16\pi}{N^2} \cdot \mathcal{R}_{loc}^0 + \frac{16\pi}{N^2} \cdot \mathcal{R}_{loc}^{ambiguity} \\ &= 12 \left(2 + \frac{m^2}{H^2} \right) \ln \left(1 + \frac{m^2}{H^2} \right) - \frac{12m^2}{H^2} + \frac{16\pi}{N^2} \cdot \mathcal{R}_{loc}^{ambiguity}, \end{aligned} \quad (4.12)$$

where

$$\frac{16\pi}{N^2} \cdot \mathcal{R}_{loc}^{ambiguity} = 24\alpha_0 + 18\alpha_1 \frac{m}{H} + 12\alpha_2 \frac{m^2}{H^2}, \quad (4.13)$$

parameterizes the scheme dependence. If we require the correct CFT limit (see (1.3)), we must set α_0 . The ambiguity then is in the choice $\{\alpha_1, \alpha_2\}$.

In fig. 8 we attempted to adjust the coefficients $\{\alpha_1, \alpha_2\}$ to match \mathcal{R}_{loc} and $\mathcal{R}_{(\mu, i\mu H/2)}^{\mathcal{N}=2^*}$ computed in section 3.2. The blue curve (left panel) represents

$$\delta\mathcal{R} = \mathcal{R}_{(\mu, i\mu H/2)}^{\mathcal{N}=2^*} - \mathcal{R}_{loc}^0, \quad (4.14)$$

and the right curve (left panel) represents the best fit to (4.14) using (4.13) with $\alpha_0 = 0$. The residual of the best fit is shown in the right panel. Clearly, the interpretation for

$$s_{ent} = s_{ent,loc}, \quad (4.15)$$

attempted in this section, is incorrect.

Acknowledgments

Research at Perimeter Institute is supported by the Government of Canada through Industry Canada and by the Province of Ontario through the Ministry of Research & Innovation. This work was further supported by NSERC through the Discovery Grants program.

A BEFP equations of motion

Within the ansatz (3.7), we obtain the following evolution and the constraint equations from (3.2):

$$\begin{aligned}
0 &= (d_+\Sigma)' + 2\Sigma' d_+ \ln \Sigma - \frac{1}{\Sigma} + \frac{\Sigma}{6} V_{BEFP}, \\
0 &= A'' - 6(\ln \Sigma)' d_+ \ln \Sigma + \frac{3}{\Sigma^2} + \frac{2(\bar{z}'d_+z + z'd_+\bar{z})}{(1-z\bar{z})^2} + 12\eta'd_+\eta - \frac{V_{BEFP}}{6}, \\
(d_+\eta)' + \left(\frac{3}{2}(\ln \Sigma)' - (\ln \eta)'\right) d_+\eta + \frac{3}{2}\eta'd_+ \ln \Sigma - \frac{\eta^2}{48}\partial_\eta V_{BEFP}, & \tag{A.1}
\end{aligned}$$

$$\begin{aligned}
0 &= (d_+\bar{z})' + \left(\frac{2z\bar{z}'}{1-z\bar{z}} + \frac{3}{2}(\ln \Sigma)'\right) d_+\bar{z} + \frac{3}{2}\bar{z}'d_+ \ln \Sigma - \frac{(1-z\bar{z})^2}{8}\partial_z V_{BEFP}, \\
0 &= (d_+z)' + \left(\frac{2\bar{z}z'}{1-z\bar{z}} + \frac{3}{2}(\ln \Sigma)'\right) d_+z + \frac{3}{2}z'd_+ \ln \Sigma - \frac{(1-z\bar{z})^2}{8}\partial_{\bar{z}} V_{BEFP},
\end{aligned}$$

$$0 = \Sigma'' + 4 \left(\frac{(\eta')^2}{\eta^2} + \frac{z'\bar{z}'}{3(1-z\bar{z})^2} \right) \Sigma, \tag{A.2}$$

$$0 = d_+^2 \Sigma - A'd_+ \Sigma + 4 \left(\frac{(d_+\eta)^2}{\eta^2} + \frac{d_+z d_+\bar{z}}{3(1-z\bar{z})^2} \right) \Sigma. \tag{A.3}$$

Taking the late-time limit, and using (3.9), we find:

$$\begin{aligned}
0 &= \eta_v'' - \frac{(\eta_v')^2}{\eta_v} + \left(\frac{3H}{2A_v} + (\ln A_v \sigma_v^3)'\right) \eta_v' - \frac{\eta_v^2}{48A_v} \partial_\eta V_{BEFP}, \\
0 &= z_v'' + \frac{2\bar{z}_v(z_v')^2}{1-z_v\bar{z}_v} + \left(\frac{3H}{2A_v} + (\ln A_v \sigma_v^3)'\right) z_v' - \frac{(1-z_v\bar{z}_v)^2}{8A_v} \partial_{\bar{z}} V_{BEFP}, \\
0 &= \bar{z}_v'' + \frac{2z_v(\bar{z}_v')^2}{1-z_v\bar{z}_v} + \left(\frac{3H}{2A_v} + (\ln A_v \sigma_v^3)'\right) \bar{z}_v' - \frac{(1-z_v\bar{z}_v)^2}{8A_v} \partial_z V_{BEFP}, \\
0 &= \sigma_v'' + \frac{4}{3}\sigma_v \left(3\frac{(\eta_v')^2}{\eta_v^2} + \frac{z_v'\bar{z}_v'}{(1-z_v\bar{z}_v)^2} \right), \\
0 &= A_v'' + 4A_v \left(3\frac{(\eta_v')^2}{\eta_v^2} + \frac{z_v'\bar{z}_v'}{(1-z_v\bar{z}_v)^2} \right) - 6A_v ((\ln \sigma_v)')^2 - 6H(\ln \sigma_v)' - \frac{1}{6}V_{BEFP}, & \tag{A.4}
\end{aligned}$$

along with the constraints

$$\begin{aligned}
0 &= \sigma'_v + \frac{\sigma_v}{2A_v}(H - A'_v), \\
0 &= \frac{(\eta'_v)^2}{\eta_v^2} + \frac{z'_v \bar{z}'_v}{3(1 - z_v \bar{z}_v)^2} - \frac{1}{2} ((\ln \sigma_v)')^2 - \frac{\sigma'_v}{4\sigma_v A_v} (3H + A'_v) - \frac{1}{24A_v} V_{BEFP}.
\end{aligned} \tag{A.5}$$

It is straightforward to verify that constraints (A.5) are consistent with (A.4).

B $(m, k) = (i\mu, \mu/2)$ equations of motion

In FG coordinate system (3.19) the gravitational equations of motion take form:

$$\begin{aligned}
0 &= z'_v + \frac{\sqrt{(\eta_v^6 \bar{z}_v^2 - \eta_v^6 + \bar{z}_v^2 + 1)(z_v^2 \eta_v^6 - \eta_v^6 + z_v^2 + 1)}(\eta_v^6 z_v - \eta_v^6 \bar{z}_v + 2z_v + 2\bar{z}_v)}{2\eta_v^2 x (\eta_v^6 \bar{z}_v^2 - \eta_v^6 + \bar{z}_v^2 + 1)}, \\
0 &= \bar{z}'_v - \frac{\sqrt{(\eta_v^6 \bar{z}_v^2 - \eta_v^6 + \bar{z}_v^2 + 1)(z_v^2 \eta_v^6 - \eta_v^6 + z_v^2 + 1)}(\eta_v^6 z_v - \eta_v^6 \bar{z}_v - 2z_v - 2\bar{z}_v)}{2\eta_v^2 x (z_v^2 \eta_v^6 - \eta_v^6 + z_v^2 + 1)}, \\
0 &= \eta'_v + \frac{\sqrt{(\eta_v^6 \bar{z}_v^2 - \eta_v^6 + \bar{z}_v^2 + 1)(z_v^2 \eta_v^6 - \eta_v^6 + z_v^2 + 1)}}{3\eta_v (z_v \bar{z}_v - 1)x}, \\
0 &= s'_v - \frac{(\eta_v^6 \bar{z}_v^2 - \eta_v^6 - 2\bar{z}_v^2 - 2)(1 + xs) \sqrt{(\eta_v^6 \bar{z}_v^2 - \eta_v^6 + \bar{z}_v^2 + 1)(\eta_v^6 z_v^2 - \eta_v^6 + z_v^2 + 1)}}{3x^2 \eta_v^2 (z_v \bar{z}_v - 1)(\eta_v^6 \bar{z}_v^2 - \eta_v^6 + \bar{z}_v^2 + 1)} - \frac{1}{x^2}.
\end{aligned} \tag{B.1}$$

This coordinate system covers the first holographic bulk subregion (see discussion in section 2.2) — from the asymptotic AdS boundary to $A_v = 0$.

C $(m, k) = (\mu, \mu/2)$ equations of motion

In FG coordinate system (3.46) the gravitational equations of motion take form:

$$\begin{aligned}
0 &= z''_{1,v} - \frac{2z_{1,v}((z'_{1,v})^2 - (z'_{2,v})^2)}{z_{2,v}^2 + z_{1,v}^2 - 1} - \frac{4z_{2,v}z'_{1,v}z'_{2,v}}{z_{2,v}^2 + z_{1,v}^2 - 1} + \frac{2z'_{1,v}}{x} \\
&\quad + \frac{h^{1/2}\eta_v^2 z_{1,v}(z_{2,v}^2(\eta_v^6 + 2) + 2z_{1,v}^2 - 2)}{2x^2(z_{2,v}^2 + z_{1,v}^2 - 1)} + \frac{5z'_{1,v}\Theta^{1/2}}{6hx\eta_v^2(z_{2,v}^2 + z_{1,v}^2 - 1)}, \\
0 &= z''_{2,v} + \frac{2z_{2,v}((z'_{1,v})^2 - (z'_{2,v})^2)}{z_{2,v}^2 + z_{1,v}^2 - 1} - \frac{4z_{1,v}z'_{1,v}z'_{2,v}}{z_{2,v}^2 + z_{1,v}^2 - 1} + \frac{2z'_{2,v}}{x} \\
&\quad + \frac{\eta_v^2 z_{2,v} h^{1/2}(\eta_v^6(z_{2,v}^2 - z_{1,v}^2 + 1) + 4z_{2,v}^2 + 4z_{1,v}^2 - 4)}{4x^2(z_{2,v}^2 + z_{1,v}^2 - 1)} + \frac{5z'_{2,v}\Theta^{1/2}}{6hx\eta_v^2(z_{2,v}^2 + z_{1,v}^2 - 1)}, \\
0 &= \eta_v'' - \frac{(\eta'_v)^2}{\eta_v} + \frac{2\eta'_v}{x} + \frac{5\eta'_v\Theta^{1/2}}{6h\eta_v^2(z_{2,v}^2 + z_{1,v}^2 - 1)x} - \frac{h^{1/2}}{6x^2\eta_v^3(z_{2,v}^2 + z_{1,v}^2 - 1)^2} \left(2z_{2,v}^2\eta_v^{12} \right. \\
&\quad \left. + ((z_{2,v}^2 + z_{1,v}^2)^2 - 1)\eta_v^6 + (z_{2,v}^2 + z_{1,v}^2 - 1)^2 \right), \\
0 &= h' + \frac{4h}{x} + \frac{2\Theta^{1/2}}{3\eta_v^2(z_{2,v}^2 + z_{1,v}^2 - 1)x}, \\
0 &= s' - h^{1/2}s,
\end{aligned} \tag{C.1}$$

where

$$\begin{aligned}
\Theta &= 12h^2x^2\eta_v^2 \left(3(z_{2,v}^2 + z_{1,v}^2 - 1)^2(\eta'_v)^2 + \eta_v^2((z'_{1,v})^2 + (z'_{2,v})^2) \right) \\
&\quad + 36\eta_v^4x^2(z_{2,v}^2 + z_{1,v}^2 - 1)^2h^3 - 3h^{5/2} \left(z_{2,v}^2\eta_v^{12} + 2((z_{2,v}^2 + z_{1,v}^2)^2 - 1)\eta_v^6 \right. \\
&\quad \left. - (z_{2,v}^2 + z_{1,v}^2 - 1)^2 \right).
\end{aligned} \tag{C.2}$$

This coordinate system covers the first holographic bulk subregion (see discussion in section 2.2) — from the asymptotic AdS boundary to $h = 0$.

D IR thermodynamics of $\mathcal{N} = 2^*$ plasma

The ratio of the bulk viscosity to the shear viscosity in $\mathcal{N} = 2^*$ plasma saturates the bulk viscosity bound [37] in the deep IR, *i.e.*,

$$\lim_{T/m \rightarrow 0} \left[\frac{\zeta}{\eta} - 2 \left(\frac{1}{3} - c_s^2 \right) \right] \approx 0, \tag{D.1}$$

as

$$\lim_{T/m \rightarrow 0} \left(\frac{1}{3} - c_s^2 \right) \approx 0.08 \approx \frac{1}{12} \quad \Longrightarrow \quad c_s^2 \rightarrow \frac{1}{4}. \quad (\text{D.2})$$

Since the bulk viscosity bound is automatically saturated for Kaluza-Klein (KK) reductions of higher dimensional conformal gauge theories to three spatial dimensions [37], (D.1) and (D.2) strongly suggests that $\mathcal{N} = 2^*$ IR thermodynamics is a KK reduction of that of emergent CFT_5 ²³. This is indeed the case [38].

Following [38], consider the $\mathcal{N} = 2^*$ vacuum in a holographic dual, the PW geometry [9]. The IR limit corresponds to $\chi \rightarrow \infty$, thus, introducing a new radial coordinate $u \rightarrow \infty$,

$$e^{2\chi} \simeq 2u, \quad e^{6\alpha} \simeq \frac{2}{3u}, \quad e^A \simeq \left(\frac{2}{3u^4} \right)^{1/3} k. \quad (\text{D.3})$$

the background metric becomes (we set the five-dimensional supergravity coupling $g = 1$)

$$ds_{PW}^2 \simeq \left(\frac{3}{2u^2} \right)^{4/3} \left[4du^2 + \left(\frac{2k}{3} \right)^2 \eta_{\mu\nu} dx^\mu dx^\nu \right]. \quad (\text{D.4})$$

The parameter k here is defined as in PW [9]. Introducing [38]

$$e^{4\phi_2} \equiv e^{2(\alpha-\chi)} \simeq \left(\frac{1}{12u^4} \right)^{1/3}, \quad e^{4\phi_1} \equiv e^{6\alpha+2\chi} \simeq \frac{4}{3}, \quad (\text{D.5})$$

the metric (D.4) can be understood as a KK reduction of the locally AdS_6 metric on a compact $x_6 \sim x_6 + L_6$:

$$ds_6^2 = e^{-2\phi_2} ds_{PW}^2 + e^{6\phi_2} dx_6^2 \simeq \frac{3^{3/2}}{2u^2} \left[4du^2 + \left(\frac{2k}{3} \right) \eta_{\mu\nu} dx^\mu dx^\nu + \frac{1}{9} dx_6^2 \right]. \quad (\text{D.6})$$

The metric (D.6) and the scalar ϕ_1 (D.5) is a solution [38] to $d = 6$ $\mathcal{N} = (1, 1)$ $F(4)$ SUGRA [39]

$$S_{F(4)} = \frac{1}{16\pi G_6} \int_{\mathcal{M}_6} d\xi^6 \sqrt{-g_6} \left(R_6 - 4(\partial\phi_1)^2 + e^{-2\phi_1} + e^{2\phi_1} - \frac{1}{6} e^{6\phi_1} \right), \quad (\text{D.7})$$

where, using the PW five-dimensional Newton's constant G_5 ,

$$\frac{L_6}{G_6} = \frac{1}{G_5} = \frac{N^2}{4\pi}. \quad (\text{D.8})$$

²³Recall that in CFT_d , $c_s^2 = \frac{1}{d-1}$.

The IR thermodynamics of $\mathcal{N} = 2^*$ plasma is thus the (appropriately rescaled) thermodynamics of AdS-Schwarzschild black branes in (D.7). Specifically,

$$(ds_6^{BH})^2 = \frac{3^{3/2}}{2u^2} \left(- \left(1 - \frac{u^5}{u_0^5} \right) (d\hat{t})^2 + d\hat{\mathbf{x}}^2 + (d\hat{x}_6)^2 + 4 \left(1 - \frac{u^5}{u_0^5} \right)^{-1} (du)^2 \right), \quad (\text{D.9})$$

where the rescaled, *i.e.*, $\hat{\cdot}$ coordinates, are related to PW coordinates x^μ and the KK direction x_6 as follows (compare with (D.6)):

$$\{\hat{t}, \hat{\mathbf{x}}\} \equiv \hat{x}^\mu = \frac{2k}{3} x^\mu, \quad \hat{x}_6 = \frac{1}{3} x_6. \quad (\text{D.10})$$

The black brane (D.9) Hawking temperature (conjugate to the PW time coordinate) is

$$T = \frac{5k}{12\pi u_0}. \quad (\text{D.11})$$

The entropy density (per unit PW volume) of the black brane (D.9) is

$$s = \frac{1}{4G_6} \frac{27}{4u_0^4} L_6 \left(\frac{2k}{3} \right)^3 \frac{1}{3} = \frac{1}{4G_5} \frac{13824\pi^4 T^4}{625k} = \frac{6912\pi^4}{625} \left(\frac{m^2}{T^2} \right)^{-1/2} \frac{T^3}{4G_5}, \quad (\text{D.12})$$

where we used the identification [10] $k = 2m$. Thus, the deep IR entropy density of $\mathcal{N} = 2^*$ plasma scales as

$$\frac{4G_5 s}{T^3} \rightarrow \frac{6912\pi^4}{625} \left(\frac{m^2}{T^2} \right)^{-1/2} \quad \text{as} \quad \frac{m^2}{T^2} \rightarrow \infty. \quad (\text{D.13})$$

References

- [1] SUPERNOVA SEARCH TEAM collaboration, A. G. Riess et al., *Observational evidence from supernovae for an accelerating universe and a cosmological constant*, *Astron. J.* **116** (1998) 1009–1038, [[astro-ph/9805201](#)].
- [2] SUPERNOVA COSMOLOGY PROJECT collaboration, S. Perlmutter et al., *Measurements of Omega and Lambda from 42 high redshift supernovae*, *Astrophys. J.* **517** (1999) 565–586, [[astro-ph/9812133](#)].
- [3] S. Kachru, R. Kallosh, A. D. Linde and S. P. Trivedi, *De Sitter vacua in string theory*, *Phys. Rev.* **D68** (2003) 046005, [[hep-th/0301240](#)].
- [4] G. Obied, H. Ooguri, L. Spodyneiko and C. Vafa, *De Sitter Space and the Swampland*, [1806.08362](#).

- [5] J. M. Maldacena, *The Large N limit of superconformal field theories and supergravity*, *Int. J. Theor. Phys.* **38** (1999) 1113–1133, [[hep-th/9711200](#)].
- [6] O. Aharony, S. S. Gubser, J. M. Maldacena, H. Ooguri and Y. Oz, *Large N field theories, string theory and gravity*, *Phys. Rept.* **323** (2000) 183–386, [[hep-th/9905111](#)].
- [7] A. Buchel and A. Karapetyan, *de Sitter Vacua of Strongly Interacting QFT*, *JHEP* **03** (2017) 114, [[1702.01320](#)].
- [8] A. Buchel, *Verlinde Gravity and AdS/CFT*, [1702.08590](#).
- [9] K. Pilch and N. P. Warner, *$N=2$ supersymmetric RG flows and the IIB dilaton*, *Nucl. Phys.* **B594** (2001) 209–228, [[hep-th/0004063](#)].
- [10] A. Buchel, A. W. Peet and J. Polchinski, *Gauge dual and noncommutative extension of an $N=2$ supergravity solution*, *Phys.Rev.* **D63** (2001) 044009, [[hep-th/0008076](#)].
- [11] N. J. Evans, C. V. Johnson and M. Petrini, *The Enhanceon and $N=2$ gauge theory: Gravity RG flows*, *JHEP* **10** (2000) 022, [[hep-th/0008081](#)].
- [12] N. Bobev, H. Elvang, D. Z. Freedman and S. S. Pufu, *Holography for $N = 2^*$ on S^4* , *JHEP* **07** (2014) 001, [[1311.1508](#)].
- [13] V. Pestun, *Localization of gauge theory on a four-sphere and supersymmetric Wilson loops*, *Commun. Math. Phys.* **313** (2012) 71–129, [[0712.2824](#)].
- [14] A. Buchel, J. G. Russo and K. Zarembo, *Rigorous Test of Non-conformal Holography: Wilson Loops in $N=2^*$ Theory*, *JHEP* **03** (2013) 062, [[1301.1597](#)].
- [15] X. Chen-Lin, J. Gordon and K. Zarembo, *$\mathcal{N} = 2^*$ super-Yang-Mills theory at strong coupling*, *JHEP* **11** (2014) 057, [[1408.6040](#)].
- [16] K. Zarembo, *Strong-Coupling Phases of Planar $N=2^*$ Super-Yang-Mills Theory*, *Theor. Math. Phys.* **181** (2014) 1522–1530, [[1410.6114](#)].
- [17] X. Chen-Lin, D. Medina-Rincon and K. Zarembo, *Quantum String Test of Nonconformal Holography*, *JHEP* **04** (2017) 095, [[1702.07954](#)].

- [18] N. Bobev, F. F. Gautason and J. Van Muiden, *Precision Holography for $\mathcal{N} = 2^*$ on S^4 from type IIB Supergravity*, *JHEP* **04** (2018) 148, [[1802.09539](#)].
- [19] J. G. Russo, E. Widn and K. Zarembo, *$N = 2$ phase transitions and holography*, *JHEP* **02** (2019) 196, [[1901.02835](#)].
- [20] A. Buchel, *Localization and holography in $N=2$ gauge theories*, *JHEP* **08** (2013) 004, [[1304.5652](#)].
- [21] I. R. Klebanov and M. J. Strassler, *Supergravity and a confining gauge theory: Duality cascades and chi SB resolution of naked singularities*, *JHEP* **08** (2000) 052, [[hep-th/0007191](#)].
- [22] P. M. Chesler and L. G. Yaffe, *Numerical solution of gravitational dynamics in asymptotically anti-de Sitter spacetimes*, *JHEP* **07** (2014) 086, [[1309.1439](#)].
- [23] I. Booth, *Black hole boundaries*, *Can. J. Phys.* **83** (2005) 1073–1099, [[gr-qc/0508107](#)].
- [24] P. Figueras, V. E. Hubeny, M. Rangamani and S. F. Ross, *Dynamical black holes and expanding plasmas*, *JHEP* **04** (2009) 137, [[0902.4696](#)].
- [25] G. Fodor, K. Nakamura, Y. Oshiro and A. Tomimatsu, *Surface gravity in dynamical spherically symmetric space-times*, *Phys. Rev.* **D54** (1996) 3882–3891, [[gr-qc/9603034](#)].
- [26] A. Buchel, *Gauge / gravity correspondence in accelerating universe*, *Phys. Rev.* **D65** (2002) 125015, [[hep-th/0203041](#)].
- [27] A. Buchel and A. A. Tseytlin, *Curved space resolution of singularity of fractional $D3$ -branes on conifold*, *Phys. Rev.* **D65** (2002) 085019, [[hep-th/0111017](#)].
- [28] A. Buchel, P. Langfelder and J. Walcher, *On time dependent backgrounds in supergravity and string theory*, *Phys. Rev.* **D67** (2003) 024011, [[hep-th/0207214](#)].
- [29] A. Buchel and A. Ghodsi, *Braneworld inflation*, *Phys. Rev.* **D70** (2004) 126008, [[hep-th/0404151](#)].

- [30] A. Buchel and D. A. Galante, *Cascading gauge theory on dS_4 and String Theory landscape*, *Nucl. Phys.* **B883** (2014) 107–148, [1310.1372].
- [31] A. Buchel, *Ringing in de Sitter spacetime*, *Nucl. Phys.* **B928** (2018) 307–320, [1707.01030].
- [32] V. Balasubramanian and A. Buchel, *On consistent truncations in $N = 2^*$ holography*, *JHEP* **02** (2014) 030, [1311.5044].
- [33] O. Aharony, A. Buchel and P. Kerner, *The Black hole in the throat: Thermodynamics of strongly coupled cascading gauge theories*, *Phys. Rev.* **D76** (2007) 086005, [0706.1768].
- [34] V. Balasubramanian, A. Buchel, S. R. Green, L. Lehner and S. L. Liebling, *Holographic Thermalization, Stability of Anti de Sitter Space, and the Fermi-Pasta-Ulam Paradox*, *Phys. Rev. Lett.* **113** (2014) 071601, [1403.6471].
- [35] L. E. Parker and D. Toms, *Quantum Field Theory in Curved Spacetime*. Cambridge Monographs on Mathematical Physics. Cambridge University Press, 2009, 10.1017/CBO9780511813924.
- [36] M. Spradlin, A. Strominger and A. Volovich, *Les Houches lectures on de Sitter space*, in *Unity from duality: Gravity, gauge theory and strings. Proceedings, NATO Advanced Study Institute, Euro Summer School, 76th session, Les Houches, France, July 30-August 31, 2001*, pp. 423–453, 2001. hep-th/0110007.
- [37] A. Buchel, *Bulk viscosity of gauge theory plasma at strong coupling*, *Phys. Lett.* **B663** (2008) 286–289, [0708.3459].
- [38] C. Hoyos, *Higher dimensional conformal field theories in the Coulomb branch*, *Phys. Lett.* **B696** (2011) 145–150, [1010.4438].
- [39] L. J. Romans, *The $F(4)$ Gauged Supergravity in Six-dimensions*, *Nucl. Phys.* **B269** (1986) 691.